Dynamics of holographic vacuum energy in the DGP model

Xing Wu,[1] Rong-Gen Cai,[2] and Zong-Hong Zhu[1,*]

[1]*Department of Astronomy, Beijing Normal University, Beijing 100875, People's Republic of China*
[2]*Institute of Theoretical Physics, Chinese Academy of Sciences, P.O. Box 2735, Beijing 100080, People's Republic of China*

We consider the evolution of the vacuum energy in the DGP model according to the holographic principle under the assumption that the relation linking the IR and UV cut-offs still holds in this scenario. The model is studied when the IR cut-off is chosen to be the Hubble scale H^{-1}, the particle horizon $R_{\rm ph}$ and the future event horizon $R_{\rm eh}$, respectively. And the two branches of the DGP model are also taken into account. Through numerical analysis, we find that in the cases of H^{-1} in the (+) branch and $R_{\rm eh}$ in both branches, the vacuum energy can play the role of dark energy. Moreover, when considering the combination of the vacuum energy and the $5D$ gravity effect in both branches, the equation of state of the effective dark energy may cross -1, which may lead to the Big Rip singularity. Besides, we constrain the model with the Type Ia supernovae and baryon oscillation data and find that our model is consistent with current data within 1σ, and that the observations prefer either a pure holographic dark energy or a pure DGP model.

PACS numbers: 98.80.-k; 98.80.Es; 04.50.-h; 95.36.+x

I. INTRODUCTION

Recent SNe Ia and WMAP observations [1, 2] have indicated that our universe is currently undergoing an accelerating expansion, which confront the fundamental theories with great challenges and also make the researches on this problem a major endeavor in modern astrophysics and cosmology. The origin of the cosmic acceleration is still a mystery and is referred to as the dark energy problem. Various models have been proposed to solve this problem. They generally fall into the following two ways. One is to add an exotic energy component with negative pressure, that is, the dark energy, to the total energy budget of the universe. Among others, the most competitive candidate of dark energy sofar is the cosmological constant due to both its theoretical simpleness and its great success in fitting with observational data, although it suffers from the cosmological constant problem[3] . Such problem is expected to be solved or alleviated in the models of dynamic dark energy (see [4] for a more detailed review), which generally contains a scalar field evolving in time and driving the acceleration, just like the scalar field introduced for the inflation stage at early universe. In fact, the cosmological constant problem is essentially a problem of quantum gravity. In quantum field theory, where the effect of gravity is neglected, the vacuum energy is determined by the UV cut-off k_c, that is $\rho_\Lambda \propto k_c^4$. No matter how we choose the UV cut-off, be it the Planck scale 10^{19}GeV or the electroweak scale TeV, the value predicted by theory is far greater that that observed $10^{-47}\mathrm{GeV}^4$. Since we are concerning problems at the cosmological scale, however, we should have take into account the effect of gravity. It is expected that the value of the cosmological constant or the vacuum energy would be predicted correctly from a complete theory of quantum gravity, which is still being explored. But at present the holographic principle, which is believed to be an important feature of quantum gravity, may shed some light on solving this problem. Follow the line of the holographic principle, the holographic dark energy model[7] is a promising candidate for solving the dark energy problem. In this model, the vacuum energy is no longer a time-independent constant, but evolves with time according to the holographic principle. The vacuum energy is related to the length measure on cosmological scale

$$\rho_\Lambda = \frac{3c^2 M_p^2}{L^2}, \tag{1}$$

where ρ_Λ is directly related to the UV cut-off, L is the IR cut-off, M_p denotes the Planck mass and c is a numerical factor by convention, which is the parameter of the model. This relation of the entanglement of UV/IR was first proposed in [8], where L was first chosen as the Hubble scale. Then Hsu[9] pointed out that this would not lead to the desired equation of state. Finally, Li[7] proposed the holographic dark energy model where L is the event horizon. And this model fits very well with current observations[16].

The other way to solve the dark energy problem is to modify the theory of gravity at large scale, without resorting to any new energy component. For example, the $f(R)$ theory[5] modifies the standard Einstein-Hilbert action to introduce an effective dark energy component in the Einstein frame. Here we focus on the DGP model [6], which describes our universe as a $4D$ brane embedded in a $5D$ Minkowski bulk and explains the origin of the dark energy as the gravity on the brane leaking into the bulk at large scale. The model is described by the action

$$S = -\frac{M_{(5)}^3}{2}\int d^5X\sqrt{-g}R_{(5)} - \frac{M_p^2}{2}\int d^4x\sqrt{-h}R_{(4)}$$

*Electronic address: zhuzh@bnu.edu.cn

$$+ \int d^4x\sqrt{-h}\mathcal{L}_m + S_{GH}, \tag{2}$$

where g_{ab} is the bulk metric and $h_{\mu\nu}$ is the induced metric on the brane. The first term contains the $5D$ Ricci scalar whereas the second term contains the $4D$ Ricci scalar on the brane, which is an extra term due to quantum effects, in contrast to the Randall-Sundrum scenario[11]. The third term represents matter localized on the brane. And S_{GH} is the Gibbsons-Hawking boundary term.

In this paper, we assume that the relation Eq.(1) still holds in the DGP model, and consider the evolution of the vacuum energy on the brane (or the brane tension) according to the holographic principle. Note that there are other models also generalizing the standard DGP model by adding a cosmological constant(LDGP)[12], a Quiessence perfect fluid(QDGP)[13], a scalar field(SDGP)[14], or the Chaplygin gas(CDGP)[15]. Although the holographic dark energy model is well consistent with observational data, it should be noted that the core of the holographic principle is that it relates the UV and IR cut-offs of a local quantum field system, which reflects some feature of quantum gravity. Thus even if the holographic vacuum energy had not played the role of dark energy, it would still be of significance to study on this problem.

The paper is organized as follows. In section II, we present the model under three cases of choosing the IR cut-off for the vacuum energy as respectively the Hubble scale H^{-1}, the particle horizon $R_{\rm ph}$ and the future event horizon $R_{\rm eh}$. We study the equation of state (EoS) of the vacuum energy and the effective EoS due to the combined effect of both the holographic vacuum energy and the 5D gravity effect. In section III, we use recent observational data to constrain the model and fit its parameters. We conclude this paper in the final section.

II. THE MODEL

We assume a flat, homogeneous and isotropic brane in accordance with the result of the WMAP observation[2]. Following [6], the Friedmann equation is

$$H^2 = (\sqrt{\frac{\rho}{3M_p^2} + \frac{1}{4r_c^2}} + \epsilon\frac{1}{2r_c})^2, \tag{3}$$

or equivalently

$$H^2 - \epsilon\frac{H}{r_c} = \frac{1}{3M_p^2}\rho, \tag{4}$$

where $H \equiv \dot{a}/a$ is the Hubble parameter and $r_c \equiv M_p^2/2M_{(5)}^3$ is the distance scale reflecting the competition between 4D and 5D effects of gravity. For $H^{-1} \ll r_c$ (early times), the 4D general relativity is recovered; for $H^{-1} \gtrsim r_c$ (late times), the 5D effect begins to be significant. $\epsilon = \pm$ represents two branches of the model of which the (+) branch is the self-accelerating solution in which the universe may enter into an accelerating phase in late time by virtue of pure 5D effect of gravity, while the (−) branch cannot undergo an acceleration without additional dark energy component. Here the vacuum energy is added in $\rho = \rho_m + \rho_\Lambda$. Obviously the dynamics is typically different from the standard FRW cosmology. In addition, we have the usual equation of conservation

$$\dot{\rho} + 3H(1+w)\rho = 0, \tag{5}$$

where w is the equation of state (EoS). Here we assume that there is no interaction between matter and vacuum energy. Therefore both components obey the equation of conservation respectively and, in particular, for matter we have $\rho_m = \rho_{m0}a^{-3}$, the same as that in usual FRW cosmology. We note that here the EoS of the vacuum energy evolves with time due to the holographic principle as shown later, as opposed to ΛCDM where $w_\Lambda \equiv -1$.

When applying the holographic principle in cosmology, a crucial problem is how to choose the IR cut-off L. In usual FRW sosmology, it is shown[7] that only in the case of choosing L as the future event horizon can vacuum energy play the role of dark energy. In the DGP framework, we consider L as the Hubble scale H^{-1}, the particle horizon $R_{\rm ph}$ and the future event horizon $R_{\rm eh}$ respectively. And then we investigate the evolution of the EoS of the vacuum energy.

Intuitionally, we may guess that for one thing, in the (-) branch where there is no self-acceleration, adding a component whose EoS $> -1/3$ will not lead to an acceleration whereas adding a dark energy component may cause the universe in this branch to accelerate; for the other thing, in the (+) branch, no matter whether the holographic vacuum energy we add can in itself play the role of dark energy, the combined effect may lead to an acceleration due to the contribution from the self-acceleration of this branch.

A. L as H^{-1}

By Eq.(1), the vacuum energy is $\rho_\Lambda = 3c^2M_p^2H^2$. For convenience we insert this result into the Friedmann Eq.(4). After defining $\Omega_m = \frac{\rho_m}{3M_p^2H_0^2} = \Omega_{m0}(1+z)^3$, $\Omega_\Lambda = \frac{\rho_\Lambda}{3M_p^2H_0^2}$, $\Omega_r = \frac{1}{4r_c^2H_0^2}$ and $\Omega_\Lambda = \frac{\rho_\Lambda}{3M_p^2H_0^2} = c^2\frac{H^2}{H_0^2}$, where H_0 is the Hubble parameter at redshift $z = 0$, the above equation can be transformed into

$$(1-c^2)(\frac{H}{H_0})^2 - 2\epsilon\sqrt{\Omega_{r_c}}\frac{H}{H_0} - \Omega_m = 0, \tag{6}$$

Then we can solve the above equation to get $E = H/H_0$.

- Case 1: $c = 1$

$$-\epsilon\frac{H}{r_c} = \frac{1}{3M_p^2}\rho_m, \tag{7}$$

where $\epsilon = +1$ corresponds to the contracting solution, and $\epsilon = -1$ represents the expanding solution

$$H = \frac{r_c}{3M_p^2}\rho_m. \tag{8}$$

In this case, the solution is easy to find by virtue of the conservation equation of ρ_m: $\rho_m \propto a^{-3}$ therefore $\rho_\Lambda \propto H^2 \propto \rho_m^2 \propto a^{-6}$, namely, the vacuum energy decreases faster than ρ_m and it cannot be dominant in late time. Thus we do not consider this case as of physical interest.

When $c \neq 1$ we write the general solution

$$\frac{H}{H_0} = \frac{\epsilon\sqrt{\Omega_{r_c}} \pm \sqrt{\Omega_{r_c} + \Omega_m(1-c^2)}}{1-c^2}. \tag{9}$$

- Case 2: $c > 1$ Since Ω_{r_c} is constant, the part under the square root on the RHS of Eq.(9) may become less than zero as z increases, therefore the solution in this case is unphysical.

- Case 3: $c < 1$ The physical solution is

$$\frac{H}{H_0} = \frac{\epsilon\sqrt{\Omega_{r_c}} + \sqrt{\Omega_{r_c} + \Omega_m(1-c^2)}}{1-c^2}. \tag{10}$$

The parameters in this expression should satisfy the following condition according to Eq.(6) at $z = 0$

$$1 - c^2 - 2\epsilon\sqrt{\Omega_{r_c}} - \Omega_{m0} = 0. \tag{11}$$

Thereby we obtain Ω_Λ and its derivative with respect to z in the following forms

$$\begin{aligned}\Omega_\Lambda &= \frac{c^2}{(1-c^2)^2}[\Omega_m(1-c^2) + 2\Omega_{r_c} \\ &+ 2\epsilon\sqrt{\Omega_{r_c}}\sqrt{\Omega_{r_c} + \Omega_m(1-c^2)}],\end{aligned} \tag{12}$$

$$\begin{aligned}\Omega'_\Lambda &= \frac{c^2}{H_0^2}2HH' \\ &= c^2\frac{\epsilon\sqrt{\Omega_{r_c}} + \sqrt{\Omega_{r_c} + \Omega_m(1-c^2)}}{1-c^2} \\ &\times \frac{3\Omega_m(1+z)^{-1}}{\sqrt{\Omega_{r_c} + \Omega_m(1-c^2)}}.\end{aligned} \tag{13}$$

Furthermore, we require that matter dominate over vacuum energy as z grows larger, or else it would spoil the success of standard Big Bang cosmology. From Eq.(12) we obtain the asymptotic expression of Ω_Λ for large z

$$\Omega_\Lambda = \frac{c^2}{1-c^2}\Omega_m. \tag{14}$$

Thus if we demand Ω_m dominate over Ω_Λ at early time, we have $\frac{c^2}{1-c^2} \ll 1$ or $c \ll 1/\sqrt{2}$. In the following we only consider the case of $c < 1/\sqrt{2} \sim 0.7$.

B. L as the particle horizon and the event horizon

The IR cut-off L is given by the definition of these two horizons

$$L = \begin{cases} R_{\rm ph} = a(t)\int_0^t \frac{dt'}{a(t')} = a\int_0^a \frac{da'}{Ha'^2} \\ \\ R_{\rm eh} = a(t)\int_t^\infty \frac{dt'}{a(t')} = a\int_a^\infty \frac{da'}{Ha'^2} \end{cases} \tag{15}$$

Here we use the Friedmann Eq.(3) and recast it into

$$E(z) = \frac{H}{H_0} = \sqrt{\Omega_m + \Omega_\Lambda + \Omega_{r_c}} + \epsilon\sqrt{\Omega_{r_c}}. \tag{16}$$

By Eq.(1) we have

$$L = \sqrt{\frac{3c^2M_p^2}{\rho_\Lambda}}. \tag{17}$$

Inserting Eq.(15) and Eq.(16) into the above equation, taking derivative with respect to a on both sides, and then using $1 + z = 1/a$, we obtain the evolution equation of Ω_Λ with respect to z [1]

$$\Omega'_\Lambda = (1+z)^{-1}\frac{2}{c}\Omega_\Lambda^{3/2}\left(\frac{\theta}{\sqrt{\Omega_m + \Omega_\Lambda + \Omega_{r_c}} + \epsilon\sqrt{\Omega_{r_c}}} + \frac{c}{\sqrt{\Omega_\Lambda}}\right), \tag{18}$$

where $\theta = +1$ corresponds to $L = R_{\rm ph}$ and $\theta = -1$ to $L = R_{\rm eh}$ and the initial condition of this differential equation is given by setting z=0 in Eq.(16)

$$\Omega_{\Lambda 0} = 1 - \epsilon 2\sqrt{\Omega_{r_c}} - \Omega_{m0}. \tag{19}$$

We can solve this equation numerically and require that, as mentioned above, Ω_Λ should become negligible compared with Ω_m as z grows.

In fact, it is only in an eternally accelerating universe that the event horizon exists. Thus, when using the event horizon as the IR cut-off, we already assume an accelerating universe and therefore the existence of some effective dark energy.

C. EoS of the vacuum energy

By energy conservation we have

$$\dot{\rho}_\Lambda + 3H(1 + w_\Lambda)\rho_\Lambda = 0, \tag{20}$$

from which we get

$$w_\Lambda = -1 - \frac{\dot{\rho_\Lambda}}{3H\rho_\Lambda} = -1 + (1+z)\frac{\Omega'_\Lambda}{3\Omega_\Lambda}, \tag{21}$$

[1] It should be noted that here we define the fractional energy densities with H_0 rather than with H, by which these fractions are often defined in literature.

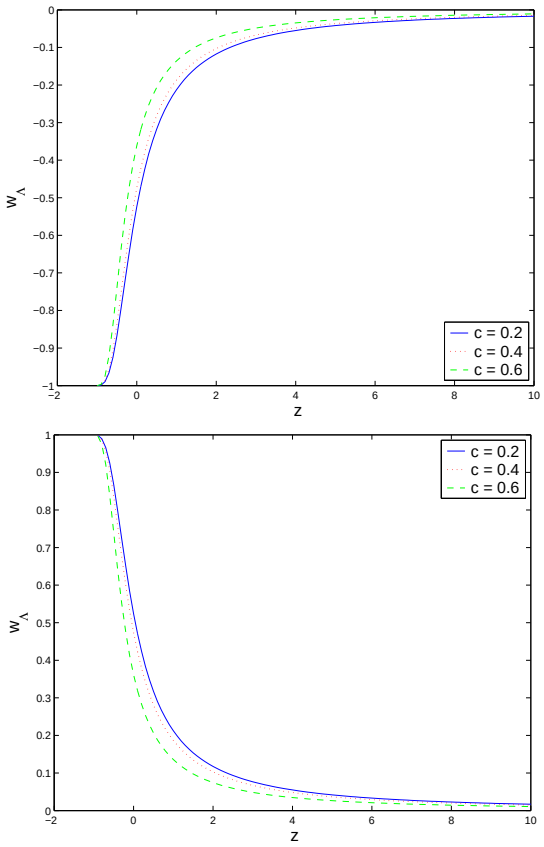

FIG. 1: The evolution of $w_\Lambda(z)$. $L = H^{-1}$ and $\Omega_m = 0.3$. In the branch $\epsilon = +1$(upper), the EoS evolves from zero in the past to -1 in the future. It is currently less than $-1/3$ and therefore Ω_Λ can serve as dark energy. In the branch $\epsilon = -1$(lower), however, the EoS is always positive.

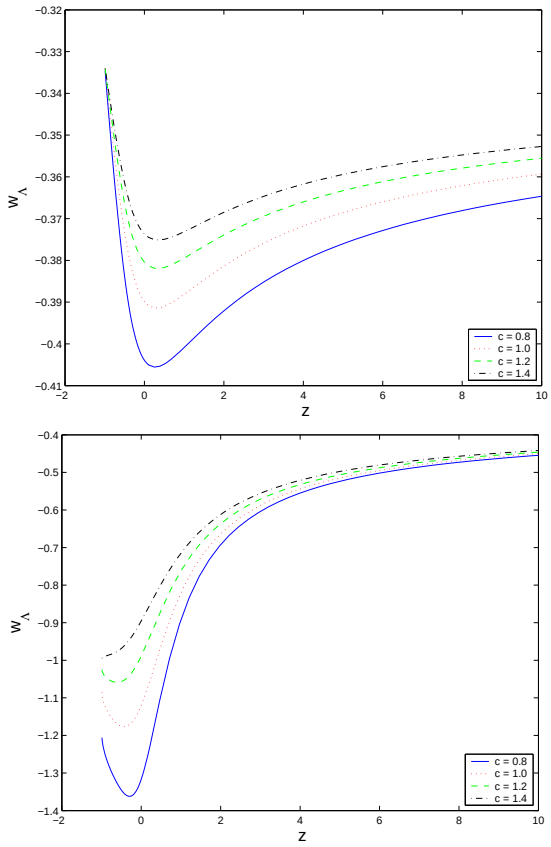

FIG. 2: The evolution of $w_\Lambda(z)$. $L = R_{\rm eh}$, $\Omega_m = 0.3$ and $\Omega_{r_c} = 0.12$. In both cases the EoS is always less than $-1/3$ and the vacuum energy can serve as dark energy. In the branch $\epsilon = +1$(upper), the EoS ends up with $-1/3$ in the future, while in the branch $\epsilon = -1$(lower) it may cross -1 for some values of the parameters.

where $1 + z = 1/a$ is used.

For L as Hubble scale, we insert Eq.(12) and Eq.(13) into (21) to get

$$w_\Lambda = -1 + \frac{1-c^2}{\epsilon\sqrt{\Omega_{r_c}} + \sqrt{\Omega_{r_c} + \Omega_m(1-c^2)}} \times \frac{\Omega_m}{\sqrt{\Omega_{r_c} + \Omega_m(1-c^2)}}, \quad (22)$$

where $c < 1$ is required. Some features of the evolution of w_Λ can be shown analytically if we rewrite this equation as

$$w_\Lambda = -1 + \frac{1}{\epsilon\sqrt{F}\sqrt{F+1} + F + 1}, \quad (23)$$

where $F \equiv \frac{\Omega_{r_c}}{\Omega_m(1-c^2)} > 0$. For $\epsilon = +1$, the denominator is always greater than 1, leading to $w_\Lambda < 0$ forever; for $\epsilon = -1$, the denominator is always less than 1, leading to $w_\Lambda > 0$. The evolution of w_Λ is shown numerically in Fig.1, where we fix $\Omega_{m0} = 0.3$ and set different values of c. From the figure we find that in the (-) branch the EoS is always positive, therefore the vacuum energy can not drive the cosmic acceleration. In the (+) branch, however, for smaller c (e.g. $c = 0.2, 0.4$ on the plot), $w_\Lambda(z = 0)$ may become less than $-1/3$ and the vacuum energy may play the role of dark energy. This is different from the case in the usual FRW universe, where H^{-1} cannot serve as the IR cut-off of the holographic dark energy.

For L as $R_{\rm ph}$ and $R_{\rm eh}$ we insert Eq.(18) into Eq.(21) to get

$$w_\Lambda = -\frac{1}{3} + \frac{2}{3c}\frac{\theta\sqrt{\Omega_\Lambda}}{\sqrt{\Omega_m + \Omega_\Lambda + \Omega_{r_c}} + \epsilon\sqrt{\Omega_{r_c}}}. \quad (24)$$

From this equation we can easily see that, it is only when $\theta = -1$ that $w_\Lambda < -\frac{1}{3}$, namely, the vacuum energy serves as dark energy if L is $R_{\rm eh}$ rather than $R_{\rm ph}$. This is the same as in the usual FRW universe. Fig.2 shows the evolution of the EoS for the case of L as $R_{\rm eh}$.

D. EoS of the effective dark energy

In order to explore the possibility of realizing accelerating expansion in our model, a combined effect of both the vacuum energy and the 5D gravity effect should be considered. That is, we need to find out the EoS of the effective dark energy. Firstly, we rewrite Eq.(16) as

$$E^2 = \Omega_m + \Omega_\Lambda + 2\Omega_{r_c} + 2\epsilon\sqrt{\Omega_{r_c}}\sqrt{\Omega_m + \Omega_\Lambda + \Omega_{r_c}}, \quad (25)$$

and then compare this expression with the Friedmann equation in usual 4D FRW cosmology consisting of a matter component and an effective dark energy

$$E^2 = \Omega_m + \Omega_{\rm eff}, \quad (26)$$

where, by the conservation equation for the effective dark energy, we have

$$\Omega_{\rm eff} = \Omega_{\rm eff}^{(0)} \exp(3\int_0^z \frac{1 + w_{\rm eff}(z')}{1+z'} dz'), \quad (27)$$

and $w_{\rm eff}$ is the EoS of the effective dark energy. We find that

$$\Omega_{\rm eff} = \Omega_\Lambda + 2\Omega_{r_c} + 2\epsilon\sqrt{\Omega_{r_c}}\sqrt{\Omega_m + \Omega_\Lambda + \Omega_{r_c}}. \quad (28)$$

Taking derivative on both sides of the above equation with respect to z, we obtain

$$1 + w_{\rm eff} = \frac{1}{3}\frac{1}{\Omega_\Lambda + 2\Omega_{r_c} + 2\epsilon\sqrt{\Omega_{r_c}}\sqrt{\Omega_m + \Omega_\Lambda + \Omega_{r_c}}} \times \left[\epsilon\sqrt{\Omega_{r_c}}\frac{3\Omega_m + \Omega'_\Lambda(1+z)}{\sqrt{\Omega_m + \Omega_\Lambda + \Omega_{r_c}}} + \Omega'_\Lambda(1+z)\right], \quad (29)$$

with the same constraint as Eq.(19). Here we also require the asymptotic behavior of $\Omega_{\rm eff}$ should be dominated over by Ω_m in the past for the same reason mentioned above.

For L as the Hubble scale, we show the evolution of the effective EoS in Fig.3 and Fig.4. Clearly in the (+) branch $w_{\rm eff}$ can become less than $-1/3$ and end up with $w_{\rm eff} = -1$, and so is $w_{\rm total}$ due to the effective dark energy dominating over matter at late time. For L as the particle horizon, Fig.5 and Fig.7 show that in the (+) branch the effective dark energy can drive the cosmic acceleration whereas it cannot in the other branch. Note that, by Fig.6, for small values of c, although the vacuum energy may serve as dark energy, it can dominate over matter as z grows and consequently spoil the BBN and structure formation. As Fig.8 and Fig.10 show, for L as the future event horizon in both branches, $w_{\rm eff}$ as well as $w_{\rm total}$ may become less than $-1/3$. Therefore in both branches acceleration may occur. Besides, there are two points worth particular mentioning: (1) From Fig.4 and Fig.7 we see that in the (-) branch, there exist a pole where $w_{\rm eff}$ diverges. This occurs because $\Omega_{\rm eff}$ evolves from positive to negative (or the opposite) as z decreases, crossing the point $\Omega_{\rm eff} = 0$ at some z^*, which implies the breakdown

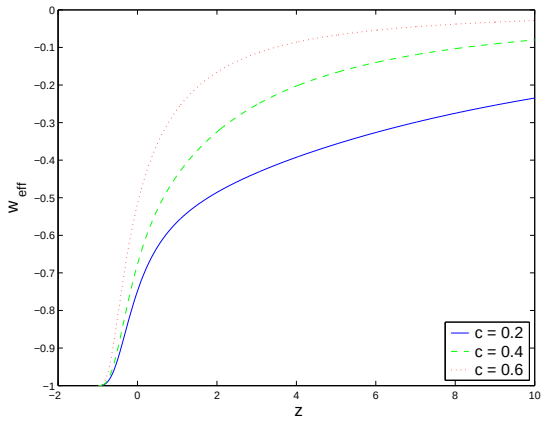

FIG. 3: The evolution of $w_{\rm eff}$. $L = H^{-1}$, $\epsilon = +1$ and $\Omega_m = 0.3$. The effective EoS may become less than $-1/3$ in the near past and end up with -1 in the future, therefore an acceleration may occur in this case.

of the effective description, rather than any pathology of the model. This can also be confirmed from the plot of $w_{\rm total}$ where the EoS is well behaved. (2) The EoS in Fig.9 to Fig.11 exhibits phantom behavior. This is because the effective dark energy posses phantom behavior and it dominates over matter at late time. Therefore $\Omega_{\rm eff}$ increases with time until the Big Rip singularity.

III. PARAMETER FITTING WITH TYPE IA SUPERNOVA OBSERVATION AND BARYON ACOUSTIC OSCILLATIONS

In this section, we confront our model with observational data and constrain the parameters. We use the SNe data compiled by Davis et al.[17], which consists of 192 SNe classified as SNIa with redshift up to $z = 1.755$. This dataset is a combination of several subsets which are 45 nearby SNe[18], 60 SNe from ESSENCE[19], 57 SNe from the Supernova Legacy Survey (SNLS)[20] and 30 high redshift SNe from Hubble Space Telescope (HST)[21], of which the data from SNLS and the nearby SNe were refitted in [19]. What the supernova observations provide is the distance modulus μ_{obj}. This quantity can be calculated from the model by

$$\mu_{th}(z; \{\theta_k\}) = 5{\rm lg}D_L(z; \{\theta_k\}) + \mathcal{M}, \quad (30)$$

where $\{\theta_k\}$ represents the parameters of the model: $\{\Omega_{m0}, c\}$ for $L = H^{-1}$, and $\{\Omega_{m0}, \Omega_{r_c}, c\}$ for $L = R_{\rm ph}$ or $R_{\rm eh}$. $\mathcal{M}$ is a nuisance parameter consisting of the Hubble constant H_0 and the absolute magnitude M

$$\mathcal{M} = M + 5{\rm lg}(\frac{c/H_0}{1Mpc}) + 25 \quad (31)$$

(here c denotes the speed of light). D_L is the dimensionless luminosity distance free of Hubble constant. In

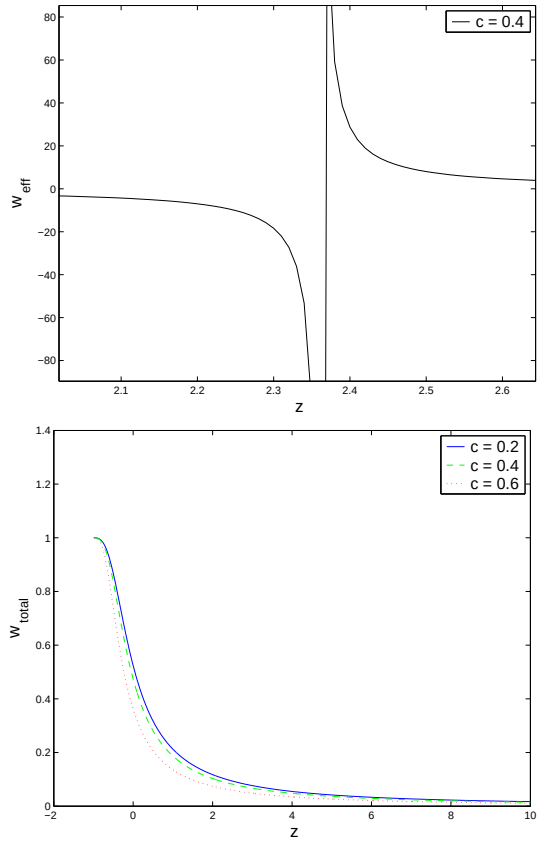

FIG. 4: The evolution of $w_{\rm eff}$(upper) and $w_{\rm total}$(lower). $L = H^{-1}$, $\epsilon = -1$ and $\Omega_m = 0.3$. There is a pole at corresponding redshift z^* where $w_{\rm eff}$ becomes divergent. This only means that the effective description breaks down around z^*, rather than that some pathology exists in the model. This can be illustrated by the plot of $w_{\rm total}$, which is well behaved.

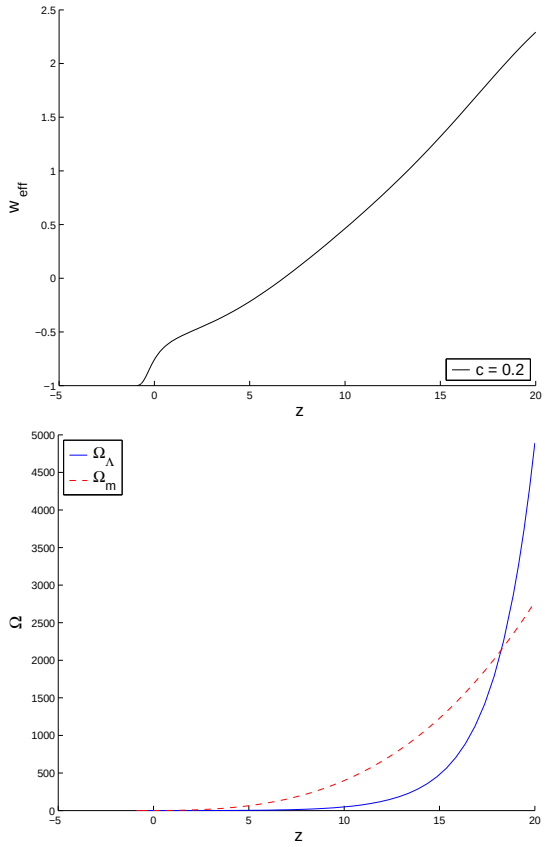

FIG. 6: The evolution of $w_{\rm eff}$. $L = R_{\rm ph}$, $\epsilon = +1$, $\Omega_m = 0.3$ and $\Omega_{r_c} = 0.12$. For $c = 0.2$ or smaller, $w_{\rm eff}$ grows larger and becomes positive (upper) at high redshift region. This implies that the vacuum energy dominates over matter as z grows larger (lower), which would violate the success of the standard Big Bang cosmology and therefore is not realistic.

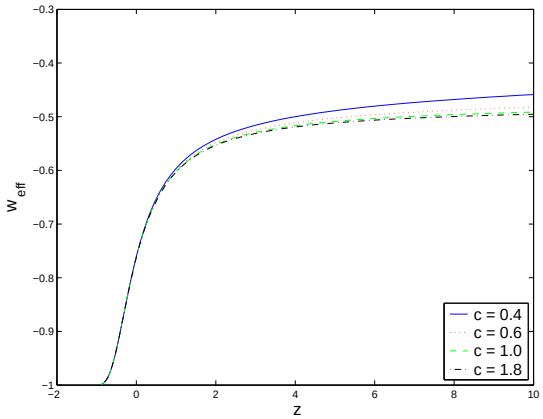

FIG. 5: The evolution of $w_{\rm eff}$. $L = R_{\rm ph}$, $\epsilon = +1$, $\Omega_m = 0.3$ and $\Omega_{r_c} = 0.12$. $w_{\rm eff}(0) < -1/3$ and an acceleration may occur. $w_{\rm eff} \to -1$ in the future and the effective dark energy ends up as a cosmological constant.

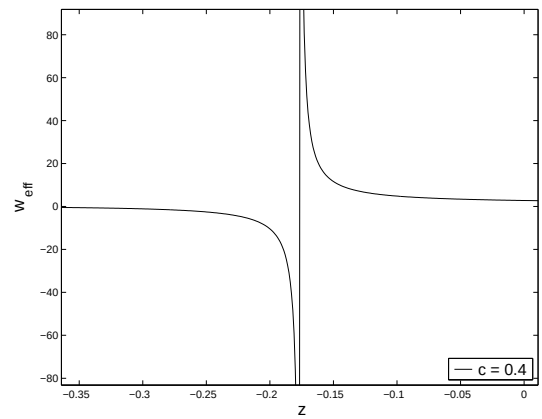

FIG. 7: The evolution of $w_{\rm eff}$. $L = R_{\rm ph}$. $\Omega_m = 0.3$, $\Omega_{r_c} = 0.12$ and $\epsilon = -1$. As the case shown in FIG.4, there exists a pole in the future evolution of the EoS, which implies the breakdown of the effective description.

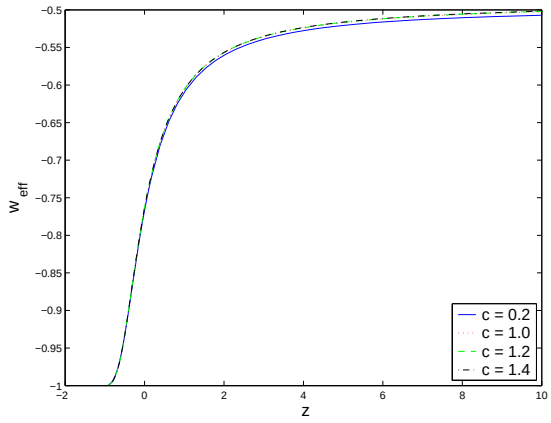

FIG. 8: The evolution of $w_{\rm eff}$. $L = R_{\rm eh}$. $\Omega_m = 0.3$, $\Omega_{r_c} = 0.12$ and $\epsilon = +1$

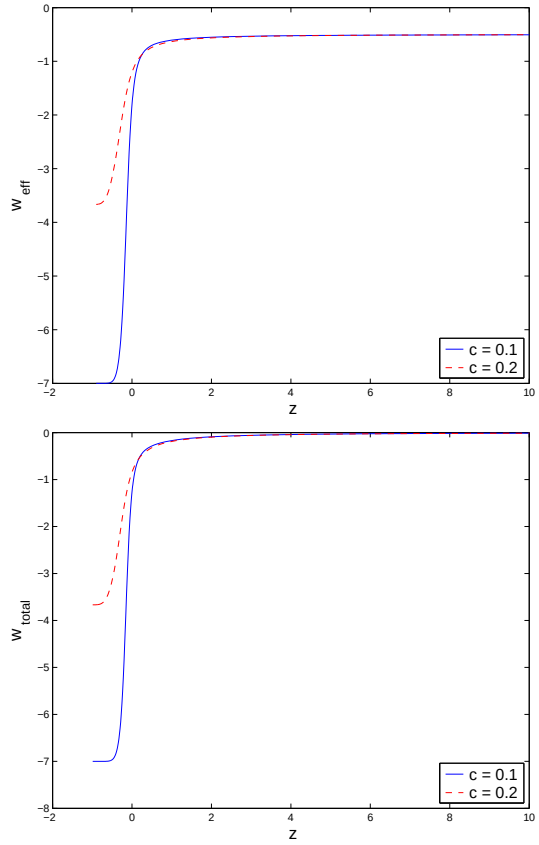

FIG. 9: The evolution of $w_{\rm eff}$. $L = R_{\rm eh}$, $\epsilon = +1$, $\Omega_m = 0.3$ and $\Omega_{r_c} = 0.06$.

a spatially flat universe it is defined by

$$D_L = (1+z)\int_0^z \frac{dz'}{E(z')}. \qquad (32)$$

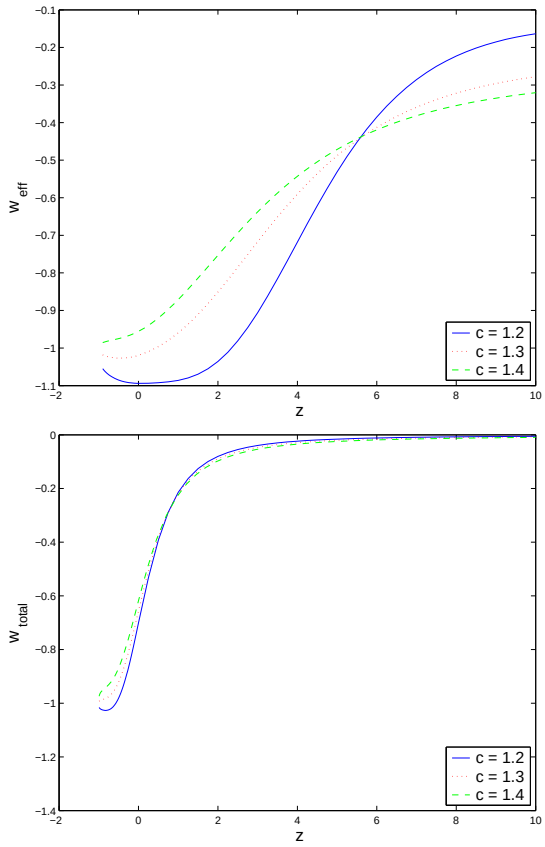

FIG. 10: The evolution of $w_{\rm eff}$. $L = R_{\rm eh}$, $\epsilon = -1$, $\Omega_m = 0.3$ and $\Omega_{r_c} = 0.12$. The effective EoS crosses -1, and since it dominates over matter in the future, the total EoS also crosses -1. This means that the future Big Rip singularity is not avoidable in this case.

The best fits are obtained by minimizing the quantity

$$\chi^2(\{\theta_k\}, \mathcal{M}) = \sum_i^{192} \frac{(\mu_{obs} - \mu_{th}(z_i; \{\theta_k\}, \mathcal{M})^2}{\sigma_i^2}, \qquad (33)$$

where σ_i are the observational uncertainties. We actually deal with the quantity χ^2 with the nuisance parameter marginalized over

$$\hat{\chi}^2 = -2\ln \int e^{-\chi^2/2} d\mathcal{M}. \qquad (34)$$

This is equivalent to minimize χ^2 with respect to $\mathcal{M}$[22], up to a negligible constant. One can easily show that χ^2 can be expanded in $\mathcal{M}$ around $\mathcal{M} = 0$ by

$$\chi^2(\{\theta_k\}, \mathcal{M}) = \chi^2(\mathcal{M} = 0, \{\theta_k\}) - 2B\mathcal{M} + C\mathcal{M}^2, \quad (35)$$

where

$$B = \sum_i^{192} \frac{\mu_{obs}(z_i) - \mu_{th}(z_i; \{\theta_k\}, \mathcal{M} = 0)}{\sigma_i^2}, \qquad (36)$$

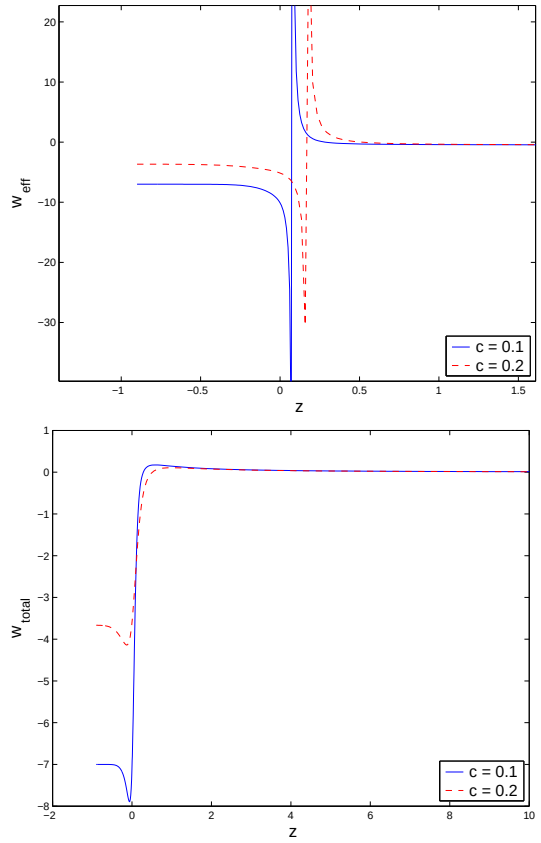

FIG. 11: The evolution of $w_{\rm eff}$. $L = R_{\rm eh}$, $\epsilon = -1$, $\Omega_m = 0.3$ and $\Omega_{r_c} = 0.06$.

$$C = \sum_i^{192} \frac{1}{\sigma_i^2}. \tag{37}$$

Obviously χ^2 becomes minimized if $\mathcal{M} = B/C$. Therefore, in practice we use

$$\chi^2_{SN}(\{\theta_k\}) = \chi^2(\mathcal{M} = 0, \{\theta_k\}) - \frac{B^2}{C} \tag{38}$$

as an alternative to $\hat{\chi}^2$ for the sake of efficiency in practical calculation without losing accuracy.

Another observational data we resort to as a complement to SNe data is from the observations of baryon acoustic oscillation peak(BAO). The acoustic oscillations in the relativistic plasma at the recombination epoch may imprint on the power spectrum of the non-relativistic matter of the late universe. And this acoustic signature in the large scale clustering of galaxies was detected by Eisenstein et al.[23] using a large sepctroscopic sample of the luminous red galaxies (LRGs) from the Sloan Digital Sky Survey (SDSS)[24]. We use the model-independent parameter A as given in[23]

$$A = \sqrt{\Omega_{m0}} z_1^{-1} [\frac{z_1}{E(z_1)} \int_0^{z_1} \frac{dz}{Ez}]^{1/3}, \tag{39}$$

where $z_1 = 0.35$ is the typical redshift of the LRGs. The measured value of A is 0.469 ± 0.017[23]. Correspondingly the quantity χ^2 is

$$\chi^2_{BAO} = \frac{(A - 0.469)^2}{0.017^2}. \tag{40}$$

And in the following we perform the joint analysis using $\chi^2 = \chi^2_{SN} + \chi^2_{BAO}$.

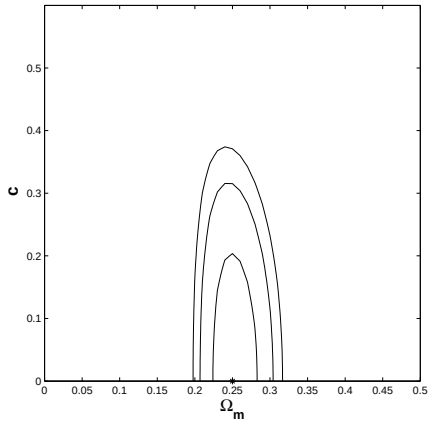

FIG. 12: Contour plot within 3σ from a joint analysis for $L = H^{-1}$ and $\epsilon = +1$. The best fits are $\Omega_{m0} = 0.25 \pm 0.02$ and $c = 0 + 0.14$.

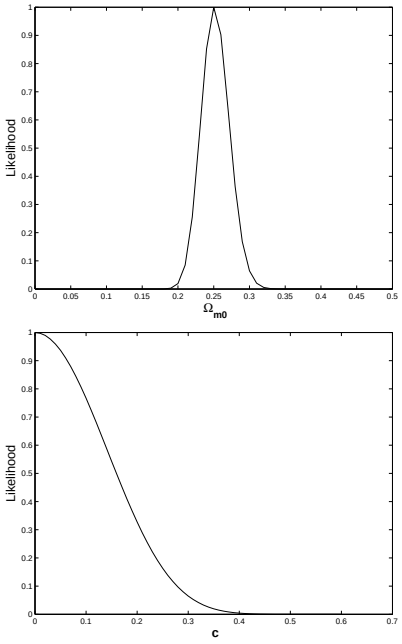

FIG. 13: Marginalized likelihood functions for Ω_{m0} and c.

For $L = H^{-1}$, there are two parameters (Ω_{m0}, c) to be fitted. And Ω_{r_c} is determined by Eq.(11). The result is shown in Fig.12. The best fits $\Omega_{m0} = 0.25$, $c = 0$

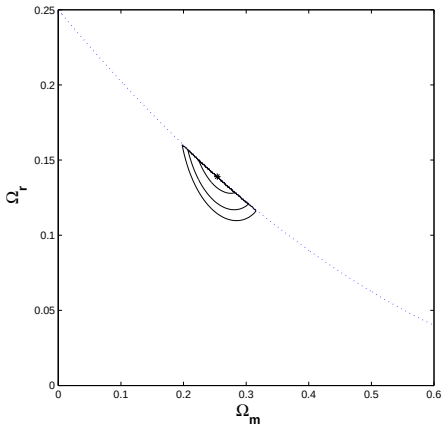

FIG. 14: Contour plot within 3σ from a joint analysis for $L = R_{\rm ph}$ and $\epsilon = +1$, with c marginalized. The best fits are $\Omega_{r_c} = 0.14 \pm 0.01$ and $\Omega_{m0} = 0.25 \pm 0.02$. The dotted line denotes the situation of $\Omega_{\Lambda 0} = 0$, above which $\Omega_{\Lambda 0} < 0$ and there the region is forbidden in our model.

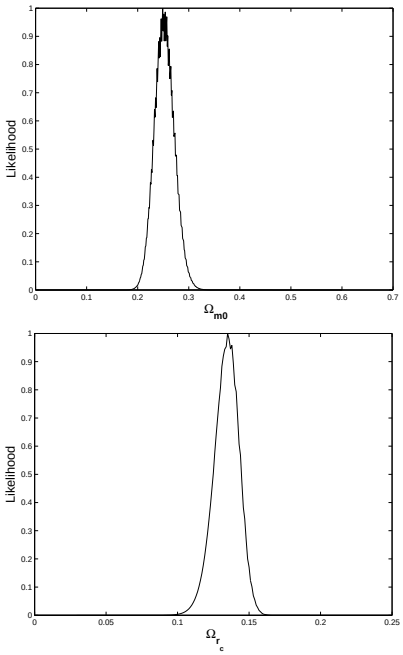

FIG. 15: Marginalized likelihood functions for Ω_{m0} and Ω_{r_c}.

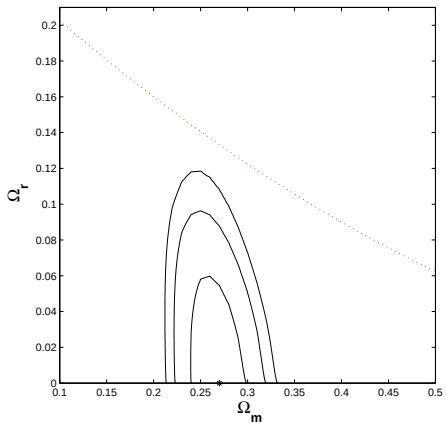

FIG. 16: Contour plot within 3σ from a joint analysis for $L = R_{\rm eh}$ and $\epsilon = +1$, with c marginalized. The best fits are $\Omega_{r_c} = 0 + 0.04$ and $\Omega_{m0} = 0.27 \pm 0.02$. Corresponding to the best fits, $c = 0.76$. Again, the dotted line denotes the boundary between $\Omega_{\Lambda 0} > 0$(below) and $\Omega_{\Lambda 0} < 0$(above).

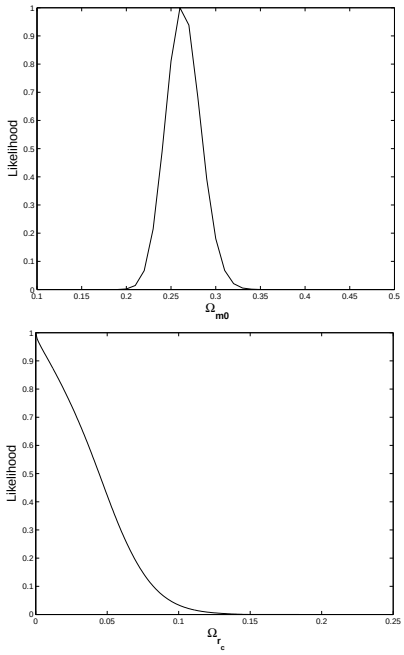

FIG. 17: Marginalized likelihood functions for Ω_{m0} and Ω_{r_c}.

and $\Omega_{r_c} = 0.14$ indicate that the observations prefer a pure DGP model without the holographic vacuum energy. This best fits are also consistent with those obtained in literature[25]. Fig.13 shows the marginalized likelihood function for the two parameters, in which the curve for Ω_{m0} is near-Gaussian whereas it is highly asymmetric for c due to the theoretical cutoff of this parameter. This leads to $\Omega_{m0} = 0.25 \pm 0.02$ and $c < 0.14$ within 68.3% confidence level.

For $L = R_{\rm ph}$, the results are given by Fig.14 and Fig.15, where we have marginalized the parameter c. In the contour plot, the dotted line represents $\Omega_{\Lambda 0} = 0$ in Eq.(19). Below this line $\Omega_{\Lambda 0} > 0$. In the region above $\Omega_{\Lambda 0} < 0$ and therefore it is the unphysical region for the parameters of the model. In the pure DGP model, the counterpart of Eq.(19) is

$$\Omega_k = 1 - 2\sqrt{\Omega_{r_c}} - \Omega_{m0}\,, \tag{41}$$

where Ω_k denotes the spatial curvature. If we identify $\Omega_{\Lambda 0}$ in Eq.(19) with Ω_k in Eq.(41), we find that our model

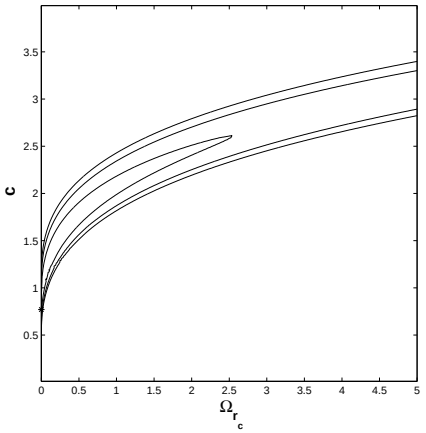

FIG. 18: Contour plot for $\Delta\chi^2 = 2.30, 6.17, 9.21$ from a joint analysis for $L = R_{\rm eh}$ and $\epsilon = -1$, with Ω_{m0} marginalized. The best fits are $\Omega_{r_c} = 0$, $c = 0.77$ denoted by a star on the plot. Corresponding to the best fits, $\Omega_{m0} = 0.27$.

TABLE I: Best fits

L	ϵ	$\Omega_{\rm m0}$	$\Omega_{\rm r_c}$	c	$w_{\rm eff0}$
H^{-1}	+1	0.25	0.14	0	-0.8000
$R_{\rm ph}$	+1	0.25	0.14	N/A	-0.7015
$R_{\rm eh}$	+1	0.27	0	0.76	-1.0828
$R_{\rm eh}$	−1	0.27	0	0.77	-1.0731

in this case is equivalent to the pure DGP model confined to a non-closed universe. The best fits are $\Omega_{r_c} = 0.14 \pm 0.01$ and $\Omega_{m0} = 0.25 \pm 0.02$, indicating a pure DGP model in a flat universe without vacuum energy.

For $L = R_{\rm eh}$, we have to consider the two branches. In the (+) branch, the results are shown in Fig.16 and Fig.17, with the parameter c marginalized. The best fits are $\Omega_{r_c} = 0 + 0.04$ and $\Omega_{m0} = 0.27 \pm 0.02$, correspondingly $c = 0.76$, indicating a pure holographic dark energy model with the negligible effect of higher dimensional gravity. In the (-) branch, as we can see from Fig.18 (with Ω_{m0} marginalized), the two outmost contours are not closed within a large region of the parameter space, indicating that current observations cannot impose tight constraint on the parameters in this case. Therefore the contours just represent the difference with respect to the minimum of χ^2, $\Delta\chi^2 = 2.30, 6.17, 9.21$ respectively, without an exact statistical meaning. Thus we do not present the likelihood plot as before. Despite of this, we can still get the best fits as $\Omega_{r_c} = 0$ and $c = 0.77$ with $\Omega_{m0} = 0.27$ correspondingly. This also indicates a pure holographic dark energy model.

IV. CONCLUSION

In this paper, we considered the evolution of the vacuum energy in the universe described by the DGP model. By numerically studying the EoS of the vacuum energy and the effective EoS of the combined effect of both vacuum energy and brane effect, we found that choosing the IR cut-off as the event horizon, the vacuum energy can drive the cosmic acceleration in both branches. In addition, the choice of the Hubble scale as the cut-off can also lead to the vacuum energy playing the role of dark energy. This is different from the case in ordinary 4D gravity, where $w_\Lambda < -1/3$ only when the event horizon is chosen as the IR cut-off. Further investigation shows that when $L = R_{\rm eh}$, the EoS may cross -1 and the vacuum energy would end up with a phantom phase, therefore the Big Rip singularity is inevitable, in contrast to the models such as LDGP[12] and SDGP[14] where only the effective EoS posses the crossing behavior and the total EoS is always larger than -1.

Through a joint analysis of SNe data and BAO data, the results of parameter fitting show that the DGP model with holographic vacuum energy can be consistent with the joint data constraints within 68.3% confidence level. For IR cut-off L as the Hubble scale and the particle horizon in the (+) branch, the best fits indicate that the observational data prefer a pure DGP model with negligible vacuum energy. For L as the event horizon in both branches, on the other hand, the best fits show a preference to the pure holographic dark energy model.

Acknowledgments

XW would like to thank Heng Yu and Xin Zhang for helpful discussions. XW and ZHZ were supported by the National Natural Science Foundation of China, under Grant No.10533010, 973 Program No.2007CB815401 and Program for New Century Excellent Talents in University (NCET) of China. RGC was supported in part by a grant from Chinese Academy of Sciences (No. KJCX3-SYW-N2), and by NSFC under grants No. 10325525, No. 10525060 and No. 90403029.

[1] A. G. Riess *et al.* [Supernova Search Team Collaboration], Astron. J. **116**, 1009 (1998) [astro-ph/9805201];
S. Perlmutter *et al.* [Supernova Cosmology ProjectCollaboration], Astrophys. J. **517**, 565 (1999) [astro-ph/9812133].

[2] D. N. Spergel *et al.* [WMAP Collaboration], [astro-ph/0603449];
L. Page *et al.* [WMAP Collaboration], [astro-ph/0603450];
G. Hinshaw *et al.* [WMAP Collaboration], [astro-ph/0603451];
N. Jarosik *et al.* [WMAP Collaboration],

[astro-ph/0603452].
[3] P. J. E. Peebles and B. Ratra, Rev. Mod. Phys. **75**, 559 (2003) [astro-ph/0207347];
S. M. Carroll, Living Rev. Rel. **4**, 1 (2001) [astro-ph/0004075];
S. Weinberg, Rev. Mod. Phys. **61**, 1 (1989).
[4] E. J. Copeland, M. Sami and S. Tsujikawa, Int. J. Mod. Phys. D **15**, 1753 (2006) [hep-th/0603057].
[5] S. Capozziello, S. Carloni and A. Troisi, [astro-ph/0303041];
S. Capozziello, V. F. Cardone, S. Carloni and A. Troisi, Int. J. Mod. Phys. D **12**, 1969 (2003);
S. M. Carroll, V. Duvvuri, M. Trodden and M. S. Turner, Phys. Rev. D **70**, 043528 (2004);
R. P. Woodard, astro-ph/0601672.
[6] G. Dvali, G. Gabadadze and M. Porrati, Phys. Lett. B **485**, 208 (2000);
G. R. Dvali, G. Gabadadze, M. Kolanovic and F. Nitti, Phys. Rev. D **64**, 084004 (2001) ;
G. R. Dvali, G. Gabadadze, M. Kolanovic and F. Nitti, Phys. Rev. D **65**, 024031 (2002).
[7] M. Li, Phys. Lett. B **603**, 1 (2004) [hep-th/0403127].
[8] A. Cohen, D.Kaplan and A. Nelson, Phys. Rev. Lett. **82**, 4971 (1999); [hep-th/9803132]
[9] S. D. H. Hsu, hep-th/0403052
[10] G. 't Hooft, [gr-qc/9310026];
L. Susskind, J. Math. Phys. 36, 6377 (1995) [hep-th/9409089]
[11] L. Randall and R. Sundrum, Phys. Rev. Lett. **83**, 4690 (1999);
L. Randall and R. Sundrum, Phys. Rev. Lett. **83**, 3370 (1999).
[12] V. Sahni and Y.Shtanov, JCAP **0311** (2003) 014 [astro-ph/0202346];
A. Lue and G. D. Starkman, Phys. Rev. D **70**, 101501 (2004) [astro-ph/0408246];
R. Lazkoz, R. Maartens and E. Majerotto, Phys. Rev. D **74**, 083510 (2006) [arXiv:astro-ph/0605701].
[13] L. P. Chimento, R. Lazkoz, R. Maartens and I. Quiros, JCAP **0609**, 004 (2006) [arXiv:astro-ph/0605450].
[14] Phys. Rev. D **75**, 023510 (2007) [astro-ph/0611834].
[15] M. Bouhmadi-López and R. Lazkoz, arXiv:0706.3896v1 [astro-ph]
[16] Q. G. Huang and Y. G. Gong, JCAP **0408**, 006 (2004) [astro-ph/0403590];
X. Zhang and F. Q. Wu, Phys. Rev. D **72**, 043524 (2005) [astro-ph/0506310];
Z. Chang, F. Q. Wu and X. Zhang, Phys. Lett. B **633**, 14 (2006) [astro-ph/0509531];
Z. L. Yi and T. J. Zhang, Mod. Phys. Lett. A **22**, 41 (2007) [astro-ph/0605596];
X. Zhang and F-Q. Wu, Phys. Rev. D **76**, 023502 (2007) [astro-ph/0701405].
[17] Davis *et al.* 2007 [astro-ph/0701510].
[18] M. Hamuy, M. M. Phillips, N. B. Suntzeff, R. A. Schommer and J. Maza, Astron. Jour. **112**, 2408 (1996) [astro-ph/9609064];
S. Jha, A. G. Riess and R. P. Kirshner, Astrophys. J. **659**, 122 (2007) [astro-ph/0612666].
[19] Wood-Vasey *et al.* 2007 [astro-ph/0701041].
[20] P. Astier *et al.*, Astron. Astrophys. **447**, 31 (2006) [arXiv:astro-ph/0510447].
[21] A. G. Riess *et al.*, Astrophys. J. **659**, 98 (2007) [arXiv:astro-ph/0611572].
[22] S. Nesseris and L. Perivolaropoulos, Phys. Rev. D **72**, 123519 (2005) [astro-ph/0511040];
L. Perivolaropoulos, Phys. Rev. D **71**, 063503 (2005) [astro-ph/0412308];
E. Di Pietro and J. F. Claeskens, Mon. Not. Roy. Astron. Soc. **341**, 1299 (2003) [astro-ph/0207332].
[23] D. J. Eisenstein, *et al.* ApJ 633, 560 (2005) [astro-ph/0501171].
[24] M. Tegmark *et al.* [SDSS Collaboration], Phys. Rev. D **69**, 103501 (2004) [astro-ph/0310723];
M. Tegmark *et al.* [SDSS Collaboration], Astrophys. J. **606**, 702 (2004) [astro-ph/0310725];
U. Seljak *et al.*, Phys. Rev. D **71**, 103515 (2005) [astro-ph/0407372];
J. K. Adelman-McCarthy *et al.* [SDSS Collaboration], Astrophys. J. Suppl. **162**, 38 (2006) [astro-ph/0507711];
K. Abazajian *et al.* [SDSS Collaboration], [astro-ph/0410239]; [astro-ph/0403325]; [astro-ph/0305492];
M. Tegmark *et al.* [SDSS Collaboration], Phys. Rev. D **74**, 123507 (2006) [astro-ph/0608632].
[25] C. Deffayet, Lett. B **502**, 199 (2001);
D. Jain, A. Dev & J. S. Alcaniz, Phys. Rev. D **66**, 083511 (2002);
J. S. Alcaniz, D. Jain & A. Dev, Phys. Rev. D **66**, 067301 (2002);
J. S. Alcaniz & Z. H. Zhu, Phys. Rev. D **71**, 083513 (2005);
Z. H. Zhu & J. S. Alcaniz, ApJ. **620**, 7 (2005);
N. Pires, Z. H. Zhu & J. S. Alcaniz, Phys. Rev. D **73**, 123530 (2006);
Z. K. Guo, Z. H. Zhu, J. S. Alcaniz & Y. Z. Zhang. ApJ. **646**, 1 (2006);
R. Maartens and E.Majerotto, Phys. Rev. D **74**, 023004 (2006) [astro-ph/0603353].

Dynamics of holographic vacuum energy in the DGP model

Xing Wu,[1,*] Rong-Gen Cai,[2,†] and Zong-Hong Zhu[1,‡]

[1]*Department of Astronomy, Beijing Normal University, Beijing 100875, People's Republic of China*
[2]*Institute of Theoretical Physics, Chinese Academy of Sciences, P.O. Box 2735, Beijing 100080, People's Republic of China*

We consider the evolution of the vacuum energy in the DGP model according to the holographic principle under the assumption that the relation linking the IR and UV cut-offs still holds in this scenario. The model is studied when the IR cut-off is chosen to be the Hubble scale H^{-1}, the particle horizon $R_{\rm ph}$ and the future event horizon $R_{\rm eh}$, respectively. And the two branches of the DGP model are also taken into account. Through numerical analysis, we find that in the cases of H^{-1} in the (+) branch and $R_{\rm eh}$ in both branches, the vacuum energy can play the role of dark energy. Moreover, when considering the combination of the vacuum energy and the $5D$ gravity effect in both branches, the equation of state of the effective dark energy may cross -1, which may lead to the Big Rip singularity. Besides, we constrain the model with the Type Ia supernovae and baryon oscillation data and find that our model is consistent with current data within 1σ, and that the observations prefer either a pure holographic dark energy or a pure DGP model.

PACS numbers: 98.80.-k; 98.80.Es; 04.50.-h; 95.36.+x

I. INTRODUCTION

Recent SNe Ia and WMAP observations [1, 2] have indicated that our universe is currently undergoing an accelerating expansion, which confront the fundamental theories with great challenges and also make the researches on this problem a major endeavor in modern astrophysics and cosmology. The origin of the cosmic acceleration is still a mystery and is referred to as the dark energy problem. Various models have been proposed to solve this problem. They generally fall into the following two ways. One is to add an exotic energy component with negative pressure, that is, the dark energy, to the total energy budget of the universe. Among others, the most competitive candidate of dark energy sofar is the cosmological constant due to both its theoretical simpleness and its great success in fitting with observational data, although it suffers from the cosmological constant problem[3] . Such problem is expected to be solved or alleviated in the models of dynamic dark energy (see [4] for a more detailed review), which generally contains a scalar field evolving in time and driving the acceleration, just like the scalar field introduced for the inflation stage at early universe. In fact, the cosmological constant problem is essentially a problem of quantum gravity. In quantum field theory, where the effect of gravity is neglected, the vacuum energy is determined by the UV cut-off k_c, that is $\rho_\Lambda \propto k_c^4$. No matter how we choose the UV cut-off, be it the Planck scale 10^{19}GeV or the electroweak scale TeV, the value predicted by theory is far greater that that observed $10^{-47}\mathrm{GeV}^4$. Since we are concerning problems at the cosmological scale, however, we should have take into account the effect of gravity. It is expected that the value of the cosmological constant or the vacuum energy would be predicted correctly from a complete theory of quantum gravity, which is still being explored. But at present the holographic principle, which is believed to be an important feature of quantum gravity, may shed some light on solving this problem. Follow the line of the holographic principle, the holographic dark energy model[7] is a promising candidate for solving the dark energy problem. In this model, the vacuum energy is no longer a time-independent constant, but evolves with time according to the holographic principle. The vacuum energy is related to the length measure on cosmological scale

$$\rho_\Lambda = \frac{3c^2 M_p^2}{L^2}, \tag{1}$$

where ρ_Λ is directly related to the UV cut-off, L is the IR cut-off, M_p denotes the Planck mass and c is a numerical factor by convention, which is the parameter of the model. This relation of the entanglement of UV/IR was first proposed in [8], where L was first chosen as the Hubble scale. Then Hsu[9] pointed out that this would not lead to the desired equation of state. Finally, Li[7] proposed the holographic dark energy model where L is the event horizon. And this model fits very well with current observations[16].

The other way to solve the dark energy problem is to modify the theory of gravity at large scale, without resorting to any new energy component. For example, the $f(R)$ theory[5] modifies the standard Einstein-Hilbert action to introduce an effective dark energy component in the Einstein frame. Here we focus on the DGP model [6], which describes our universe as a $4D$ brane embedded in a $5D$ Minkowski bulk and explains the origin of the dark energy as the gravity on the brane leaking into the bulk at large scale. The model is described by the action

*Electronic address: wxxwwxxw@mail.bnu.edu.cn
†Electronic address: cairg@itp.ac.cn
‡Electronic address: zhuzh@bnu.edu.cn

$$S = -\frac{M_{(5)}^3}{2}\int d^5X\sqrt{-g}R_{(5)} - \frac{M_p^2}{2}\int d^4x\sqrt{-h}R_{(4)} + \int d^4x\sqrt{-h}\mathcal{L}_m + S_{GH}, \quad (2)$$

where g_{ab} is the bulk metric and $h_{\mu\nu}$ is the induced metric on the brane. The first term contains the $5D$ Ricci scalar whereas the second term contains the $4D$ Ricci scalar on the brane, which is an extra term due to quantum effects, in contrast to the Randall-Sundrum scenario[11]. The third term represents matter localized on the brane. And S_{GH} is the Gibbsons-Hawking boundary term.

In this paper, we assume that the relation Eq.(1) still holds in the DGP model, and consider the evolution of the vacuum energy on the brane (or the brane tension) according to the holographic principle. Note that there are other models also generalizing the standard DGP model by adding a cosmological constant(LDGP)[12], a Quiessence perfect fluid(QDGP)[13], a scalar field(SDGP)[14], or the Chaplygin gas(CDGP)[15]. Although the holographic dark energy model is well consistent with observational data, it should be noted that the core of the holographic principle is that it relates the UV and IR cut-offs of a local quantum field system, which reflects some feature of quantum gravity. Thus even if the holographic vacuum energy had not played the role of dark energy, it would still be of significance to study on this problem.

The paper is organized as follows. In section II, we present the model under three cases of choosing the IR cut-off for the vacuum energy as respectively the Hubble scale H^{-1}, the particle horizon $R_{\rm ph}$ and the future event horizon $R_{\rm eh}$. We study the equation of state (EoS) of the vacuum energy and the effective EoS due to the combined effect of both the holographic vacuum energy and the 5D gravity effect. In section III, we use recent observational data to constrain the model and fit its parameters. We conclude this paper in the final section.

II. THE MODEL

We assume a flat, homogeneous and isotropic brane in accordance with the result of the WMAP observation[2]. Following [6], the Friedmann equation is

$$H^2 = (\sqrt{\frac{\rho}{3M_p^2} + \frac{1}{4r_c^2}} + \epsilon\frac{1}{2r_c})^2, \quad (3)$$

or equivalently

$$H^2 - \epsilon\frac{H}{r_c} = \frac{1}{3M_p^2}\rho, \quad (4)$$

where $H \equiv \dot{a}/a$ is the Hubble parameter and $r_c \equiv M_p^2/2M_{(5)}^3$ is the distance scale reflecting the competition between 4D and 5D effects of gravity. For $H^{-1} \ll r_c$ (early times), the 4D general relativity is recovered; for $H^{-1} \gtrsim r_c$ (late times), the 5D effect begins to be significant. $\epsilon = \pm$ represents two branches of the model of which the (+) branch is the self-accelerating solution in which the universe may enter into an accelerating phase in late time by virtue of pure 5D effect of gravity, while the (−) branch cannot undergo an acceleration without additional dark energy component. Here the vacuum energy is added in $\rho = \rho_m + \rho_\Lambda$. Obviously the dynamics is typically different from the standard FRW cosmology. In addition, we have the usual equation of conservation

$$\dot{\rho} + 3H(1+w)\rho = 0, \quad (5)$$

where w is the equation of state (EoS). Here we assume that there is no interaction between matter and vacuum energy. Therefore both components obey the equation of conservation respectively and, in particular, for matter we have $\rho_m = \rho_{m0}a^{-3}$, the same as that in usual FRW cosmology. We note that here the EoS of the vacuum energy evolves with time due to the holographic principle as shown later, as opposed to ΛCDM where $w_\Lambda \equiv -1$.

When applying the holographic principle in cosmology, a crucial problem is how to choose the IR cut-off L. In usual FRW sosmology, it is shown[7] that only in the case of choosing L as the future event horizon can vacuum energy play the role of dark energy. In the DGP framework, we consider L as the Hubble scale H^{-1}, the particle horizon $R_{\rm ph}$ and the future event horizon $R_{\rm eh}$ respectively. And then we investigate the evolution of the EoS of the vacuum energy.

Intuitionally, we may guess that for one thing, in the (-) branch where there is no self-acceleration, adding a component whose EoS $> -1/3$ will not lead to an acceleration whereas adding a dark energy component may cause the universe in this branch to accelerate; for the other thing, in the (+) branch, no matter whether the holographic vacuum energy we add can in itself play the role of dark energy, the combined effect may lead to an acceleration due to the contribution from the self-acceleration of this branch.

A. L as H^{-1}

By Eq.(1), the vacuum energy is $\rho_\Lambda = 3c^2M_p^2H^2$. For convenience we insert this result into the Friedmann Eq.(4). After defining $\Omega_m = \frac{\rho_m}{3M_p^2H_0^2} = \Omega_{m0}(1+z)^3$, $\Omega_\Lambda = \frac{\rho_\Lambda}{3M_p^2H_0^2}$, $\Omega_r = \frac{1}{4r_c^2H_0^2}$ and $\Omega_\Lambda = \frac{\rho_\Lambda}{3M_p^2H_0^2} = c^2\frac{H^2}{H_0^2}$, where H_0 is the Hubble parameter at redshift $z = 0$, the above equation can be transformed into

$$(1-c^2)(\frac{H}{H_0})^2 - 2\epsilon\sqrt{\Omega_{r_c}}\frac{H}{H_0} - \Omega_m = 0, \quad (6)$$

Then we can solve the above equation to get $E = H/H_0$.

- Case 1: $c = 1$

$$-\epsilon\frac{H}{r_c} = \frac{1}{3M_p^2}\rho_m, \quad (7)$$

where $\epsilon = +1$ corresponds to the contracting solution, and $\epsilon = -1$ represents the expanding solution

$$H = \frac{r_c}{3M_p^2}\rho_m. \tag{8}$$

In this case, the solution is easy to find by virtue of the conservation equation of ρ_m: $\rho_m \propto a^{-3}$ therefore $\rho_\Lambda \propto H^2 \propto \rho_m^2 \propto a^{-6}$, namely, the vacuum energy decreases faster than ρ_m and it cannot be dominant in late time. Thus we do not consider this case as of physical interest.

When $c \neq 1$ we write the general solution

$$\frac{H}{H_0} = \frac{\epsilon\sqrt{\Omega_{r_c}} \pm \sqrt{\Omega_{r_c} + \Omega_m(1-c^2)}}{1-c^2}. \tag{9}$$

- Case 2: $c > 1$ Since Ω_{r_c} is constant, the part under the square root on the RHS of Eq.(9) may become less than zero as z increases, therefore the solution in this case is unphysical.

- Case 3: $c < 1$ The physical solution is

$$\frac{H}{H_0} = \frac{\epsilon\sqrt{\Omega_{r_c}} + \sqrt{\Omega_{r_c} + \Omega_m(1-c^2)}}{1-c^2}. \tag{10}$$

The parameters in this expression should satisfy the following condition according to Eq.(6) at $z = 0$

$$1 - c^2 - 2\epsilon\sqrt{\Omega_{r_c}} - \Omega_{m0} = 0. \tag{11}$$

Thereby we obtain Ω_Λ and its derivative with respect to z in the following forms

$$\begin{aligned}\Omega_\Lambda &= \frac{c^2}{(1-c^2)^2}[\Omega_m(1-c^2) + 2\Omega_{r_c} \\ &+ 2\epsilon\sqrt{\Omega_{r_c}}\sqrt{\Omega_{r_c} + \Omega_m(1-c^2)}],\end{aligned} \tag{12}$$

$$\begin{aligned}\Omega'_\Lambda &= \frac{c^2}{H_0^2}2HH' \\ &= c^2\frac{\epsilon\sqrt{\Omega_{r_c}} + \sqrt{\Omega_{r_c} + \Omega_m(1-c^2)}}{1-c^2} \\ &\times \frac{3\Omega_m(1+z)^{-1}}{\sqrt{\Omega_{r_c} + \Omega_m(1-c^2)}}.\end{aligned} \tag{13}$$

Furthermore, we require that matter dominate over vacuum energy as z grows larger, or else it would spoil the success of standard Big Bang cosmology. From Eq.(12) we obtain the asymptotic expression of Ω_Λ for large z

$$\Omega_\Lambda = \frac{c^2}{1-c^2}\Omega_m. \tag{14}$$

Thus if we demand Ω_m dominate over Ω_Λ at early time, we have $\frac{c^2}{1-c^2} \ll 1$ or $c \ll 1/\sqrt{2}$. In the following we only consider the case of $c < 1/\sqrt{2} \sim 0.7$.

B. L as the particle horizon and the event horizon

The IR cut-off L is given by the definition of these two horizons

$$L = \begin{cases} R_{\rm ph} = a(t)\int_0^t \frac{dt'}{a(t')} = a\int_0^a \frac{da'}{Ha'^2} \\ \\ R_{\rm eh} = a(t)\int_t^\infty \frac{dt'}{a(t')} = a\int_a^\infty \frac{da'}{Ha'^2} \end{cases} \tag{15}$$

Here we use the Friedmann Eq.(3) and recast it into

$$E(z) = \frac{H}{H_0} = \sqrt{\Omega_m + \Omega_\Lambda + \Omega_{r_c}} + \epsilon\sqrt{\Omega_{r_c}}. \tag{16}$$

By Eq.(1) we have

$$L = \sqrt{\frac{3c^2M_p^2}{\rho_\Lambda}}. \tag{17}$$

Inserting Eq.(15) and Eq.(16) into the above equation, taking derivative with respect to a on both sides, and then using $1 + z = 1/a$, we obtain the evolution equation of Ω_Λ with respect to z [1]

$$\Omega'_\Lambda = (1+z)^{-1}\frac{2}{c}\Omega_\Lambda^{3/2}\left(\frac{\theta}{\sqrt{\Omega_m + \Omega_\Lambda + \Omega_{r_c}} + \epsilon\sqrt{\Omega_{r_c}}} + \frac{c}{\sqrt{\Omega_\Lambda}}\right), \tag{18}$$

where $\theta = +1$ corresponds to $L = R_{\rm ph}$ and $\theta = -1$ to $L = R_{\rm eh}$ and the initial condition of this differential equation is given by setting z=0 in Eq.(16)

$$\Omega_{\Lambda 0} = 1 - \epsilon 2\sqrt{\Omega_{r_c}} - \Omega_{m0}. \tag{19}$$

We can solve this equation numerically and require that, as mentioned above, Ω_Λ should become negligible compared with Ω_m as z grows.

In fact, it is only in an eternally accelerating universe that the event horizon exists. Thus, when using the event horizon as the IR cut-off, we already assume an accelerating universe and therefore the existence of some effective dark energy.

C. EoS of the vacuum energy

By energy conservation we have

$$\dot{\rho}_\Lambda + 3H(1 + w_\Lambda)\rho_\Lambda = 0, \tag{20}$$

from which we get

$$w_\Lambda = -1 - \frac{\dot{\rho_\Lambda}}{3H\rho_\Lambda} = -1 + (1+z)\frac{\Omega'_\Lambda}{3\Omega_\Lambda}, \tag{21}$$

[1] It should be noted that here we define the fractional energy densities with H_0 rather than with H, by which these fractions are often defined in literature.

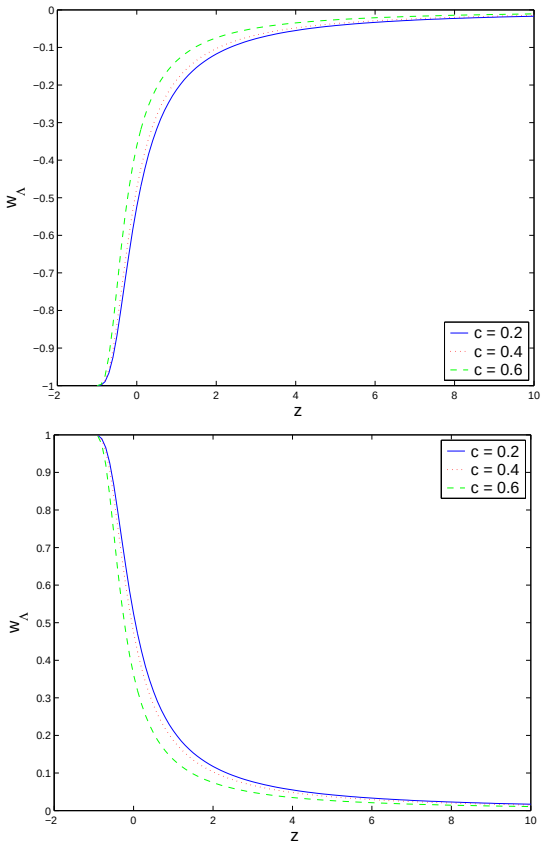

FIG. 1: The evolution of $w_\Lambda(z)$. $L = H^{-1}$ and $\Omega_m = 0.3$. In the branch $\epsilon = +1$(top), the EoS evolves from zero in the past to -1 in the future. It is currently less than $-1/3$ and therefore Ω_Λ can serve as dark energy. In the branch $\epsilon = -1$(bottom), however, the EoS is always positive.

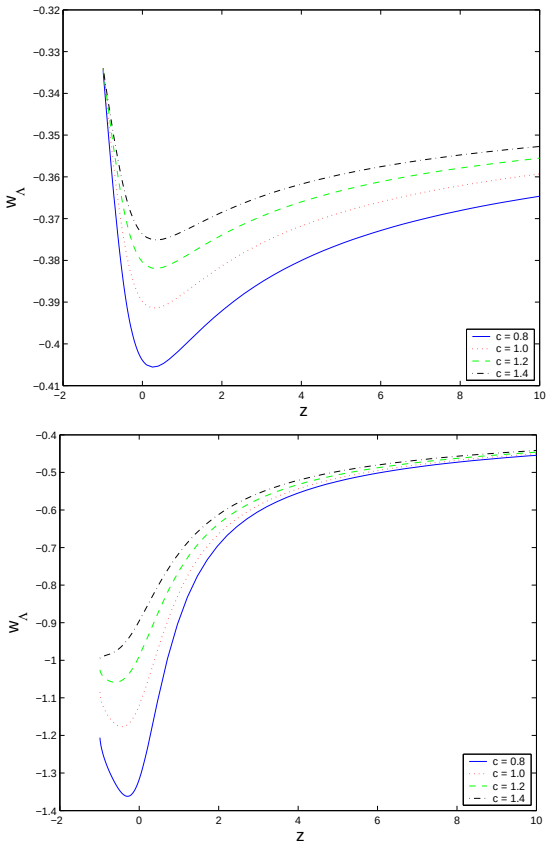

FIG. 2: The evolution of $w_\Lambda(z)$. $L = R_{\rm eh}$, $\Omega_m = 0.3$ and $\Omega_{r_c} = 0.12$. In both cases the EoS is always less than $-1/3$ and the vacuum energy can serve as dark energy. In the branch $\epsilon = +1$(top), the EoS ends up with $-1/3$ in the future, while in the branch $\epsilon = -1$(bottom) it may cross -1 for some values of the parameters.

where $1 + z = 1/a$ is used.

For L as Hubble scale, we insert Eq.(12) and Eq.(13) into (21) to get

$$w_\Lambda = -1 + \frac{1-c^2}{\epsilon\sqrt{\Omega_{r_c}} + \sqrt{\Omega_{r_c} + \Omega_m(1-c^2)}} \times \frac{\Omega_m}{\sqrt{\Omega_{r_c} + \Omega_m(1-c^2)}}, \quad (22)$$

where $c < 1$ is required. Some features of the evolution of w_Λ can be shown analytically if we rewrite this equation as

$$w_\Lambda = -1 + \frac{1}{\epsilon\sqrt{F}\sqrt{F+1} + F + 1}, \quad (23)$$

where $F \equiv \frac{\Omega_{r_c}}{\Omega_m(1-c^2)} > 0$. For $\epsilon = +1$, the denominator is always greater than 1, leading to $w_\Lambda < 0$ forever; for $\epsilon = -1$, the denominator is always less than 1, leading to $w_\Lambda > 0$. The evolution of w_Λ is shown numerically in Fig.1, where we fix $\Omega_{m0} = 0.3$ and set different values of c. From the figure we find that in the (-) branch the EoS is always positive, therefore the vacuum energy can not drive the cosmic acceleration. In the (+) branch, however, for smaller c (e.g. $c = 0.2, 0.4$ on the plot), $w_\Lambda(z = 0)$ may become less than $-1/3$ and the vacuum energy may play the role of dark energy. This is different from the case in the usual FRW universe, where H^{-1} cannot serve as the IR cut-off of the holographic dark energy.

For L as $R_{\rm ph}$ and $R_{\rm eh}$ we insert Eq.(18) into Eq.(21) to get

$$w_\Lambda = -\frac{1}{3} + \frac{2}{3c}\frac{\theta\sqrt{\Omega_\Lambda}}{\sqrt{\Omega_m + \Omega_\Lambda + \Omega_{r_c}} + \epsilon\sqrt{\Omega_{r_c}}}. \quad (24)$$

From this equation we can easily see that, it is only when $\theta = -1$ that $w_\Lambda < -\frac{1}{3}$, namely, the vacuum energy serves as dark energy if L is $R_{\rm eh}$ rather than $R_{\rm ph}$. This is the same as in the usual FRW universe. Fig.2 shows the evolution of the EoS for the case of L as $R_{\rm eh}$.

D. EoS of the effective dark energy

In order to explore the possibility of realizing accelerating expansion in our model, a combined effect of both the vacuum energy and the 5D gravity effect should be considered. That is, we need to find out the EoS of the effective dark energy. Firstly, we rewrite Eq.(16) as

$$E^2 = \Omega_m + \Omega_\Lambda + 2\Omega_{r_c} + 2\epsilon\sqrt{\Omega_{r_c}}\sqrt{\Omega_m + \Omega_\Lambda + \Omega_{r_c}}, \quad (25)$$

and then compare this expression with the Friedmann equation in usual 4D FRW cosmology consisting of a matter component and an effective dark energy

$$E^2 = \Omega_m + \Omega_{\rm eff}, \quad (26)$$

where, by the conservation equation for the effective dark energy, we have

$$\Omega_{\rm eff} = \Omega_{\rm eff}^{(0)} \exp(3\int_0^z \frac{1 + w_{\rm eff}(z')}{1+z'} dz'), \quad (27)$$

and $w_{\rm eff}$ is the EoS of the effective dark energy. We find that

$$\Omega_{\rm eff} = \Omega_\Lambda + 2\Omega_{r_c} + 2\epsilon\sqrt{\Omega_{r_c}}\sqrt{\Omega_m + \Omega_\Lambda + \Omega_{r_c}}. \quad (28)$$

Taking derivative on both sides of the above equation with respect to z, we obtain

$$1 + w_{\rm eff} = \frac{1}{3}\frac{1}{\Omega_\Lambda + 2\Omega_{r_c} + 2\epsilon\sqrt{\Omega_{r_c}}\sqrt{\Omega_m + \Omega_\Lambda + \Omega_{r_c}}} \times \left[\epsilon\sqrt{\Omega_{r_c}}\frac{3\Omega_m + \Omega'_\Lambda(1+z)}{\sqrt{\Omega_m + \Omega_\Lambda + \Omega_{r_c}}} + \Omega'_\Lambda(1+z)\right], \quad (29)$$

with the same constraint as Eq.(19). Here we also require the asymptotic behavior of $\Omega_{\rm eff}$ should be dominated over by Ω_m in the past for the same reason mentioned above.

For L as the Hubble scale, we show the evolution of the effective EoS in Fig.3 and Fig.4. Clearly in the (+) branch $w_{\rm eff}$ can become less than $-1/3$ and end up with $w_{\rm eff} = -1$, and so is $w_{\rm total}$ due to the effective dark energy dominating over matter at late time. For L as the particle horizon, Fig.5 and Fig.7 show that in the (+) branch the effective dark energy can drive the cosmic acceleration whereas it cannot in the other branch. Note that, by Fig.6, for small values of c, although the vacuum energy may serve as dark energy, it can dominate over matter as z grows and consequently spoil the BBN and structure formation. As Fig.8 and Fig.10 show, for L as the future event horizon in both branches, $w_{\rm eff}$ as well as $w_{\rm total}$ may become less than $-1/3$. Therefore in both branches acceleration may occur. Besides, there are two points worth particular mentioning: (1) From Fig.4 and Fig.7 we see that in the (-) branch, there exist a pole where $w_{\rm eff}$ diverges. This occurs because $\Omega_{\rm eff}$ evolves from positive to negative (or the opposite) as z decreases, crossing the point $\Omega_{\rm eff} = 0$ at some z^*, which implies the breakdown

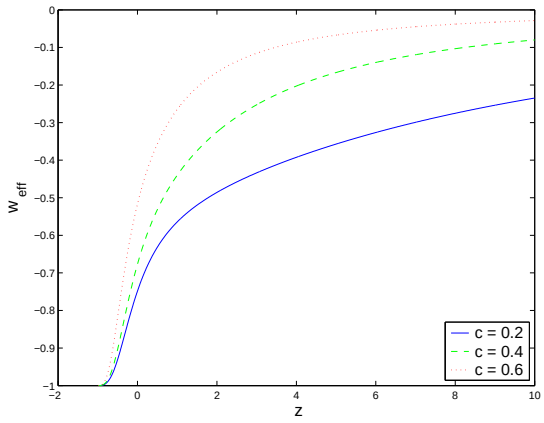

FIG. 3: The evolution of $w_{\rm eff}$. $L = H^{-1}$, $\epsilon = +1$ and $\Omega_m = 0.3$. The effective EoS may become less than $-1/3$ in the near past and end up with -1 in the future, therefore an acceleration may occur in this case.

of the effective description, rather than any pathology of the model. This can also be confirmed from the plot of $w_{\rm total}$ where the EoS is well behaved. (2) The EoS in Fig.9 to Fig.11 exhibits phantom behavior. This is because the effective dark energy posses phantom behavior and it dominates over matter at late time. Therefore $\Omega_{\rm eff}$ increases with time until the Big Rip singularity.

III. PARAMETER FITTING WITH TYPE IA SUPERNOVA OBSERVATION AND BARYON ACOUSTIC OSCILLATIONS

In this section, we confront our model with observational data and constrain the parameters. We use the SNe data compiled by Davis et al.[17], which consists of 192 SNe classified as SNIa with redshift up to $z = 1.755$. This dataset is a combination of several subsets which are 45 nearby SNe[18], 60 SNe from ESSENCE[19], 57 SNe from the Supernova Legacy Survey (SNLS)[20] and 30 high redshift SNe from Hubble Space Telescope (HST)[21], of which the data from SNLS and the nearby SNe were refitted in [19]. What the supernova observations provide is the distance modulus μ_{obj}. This quantity can be calculated from the model by

$$\mu_{th}(z; \{\theta_k\}) = 5{\rm lg}D_L(z; \{\theta_k\}) + \mathcal{M}, \quad (30)$$

where $\{\theta_k\}$ represents the parameters of the model: $\{\Omega_{m0}, c\}$ for $L = H^{-1}$, and $\{\Omega_{m0}, \Omega_{r_c}, c\}$ for $L = R_{\rm ph}$ or $R_{\rm eh}$. $\mathcal{M}$ is a nuisance parameter consisting of the Hubble constant H_0 and the absolute magnitude M

$$\mathcal{M} = M + 5{\rm lg}(\frac{c/H_0}{1Mpc}) + 25 \quad (31)$$

(here c denotes the speed of light). D_L is the dimensionless luminosity distance free of Hubble constant. In

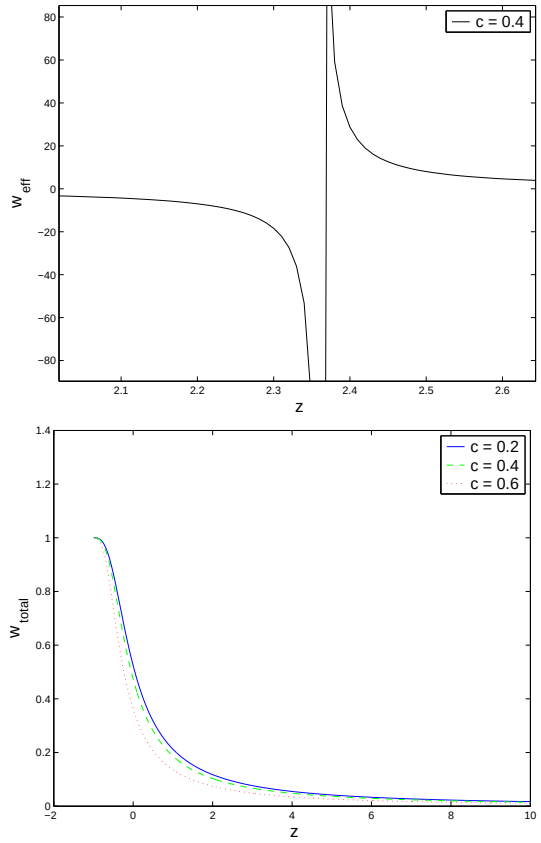

FIG. 4: The evolution of $w_{\rm eff}$(top) and $w_{\rm total}$(bottom). $L = H^{-1}$, $\epsilon = -1$ and $\Omega_m = 0.3$. There is a pole at corresponding redshift z^* where $w_{\rm eff}$ becomes divergent. This only means that the effective description breaks down around z^*, rather than that some pathology exists in the model. This can be illustrated by the plot of $w_{\rm total}$, which is well behaved.

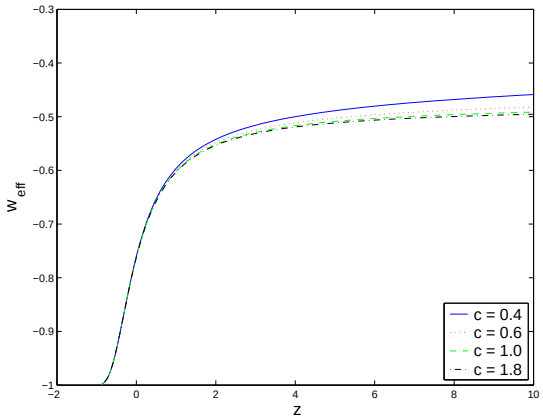

FIG. 5: The evolution of $w_{\rm eff}$. $L = R_{\rm ph}$, $\epsilon = +1$, $\Omega_m = 0.3$ and $\Omega_{r_c} = 0.12$. $w_{\rm eff}(0) < -1/3$ and an acceleration may occur. $w_{\rm eff} \to -1$ in the future and the effective dark energy ends up as a cosmological constant.

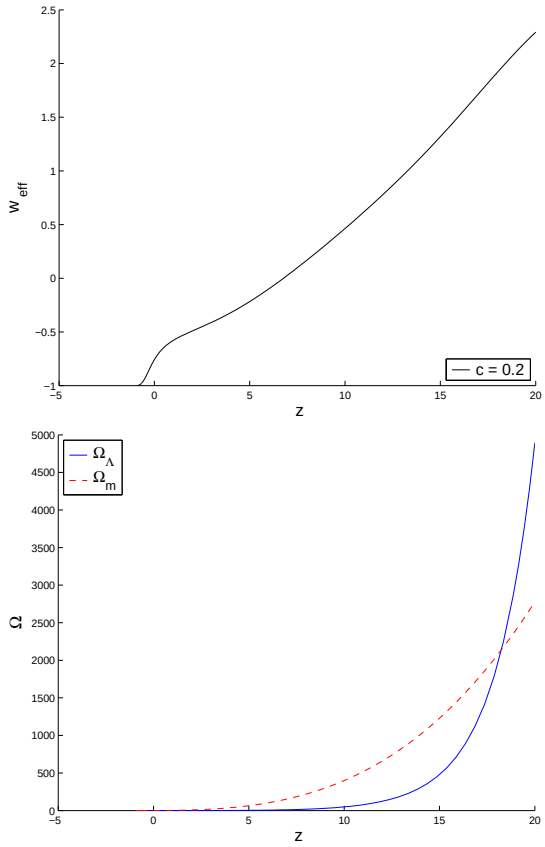

FIG. 6: The evolution of $w_{\rm eff}$. $L = R_{\rm ph}$, $\epsilon = +1$, $\Omega_m = 0.3$ and $\Omega_{r_c} = 0.12$. For $c = 0.2$ or smaller, $w_{\rm eff}$ grows larger and becomes positive (top) at high redshift region. This implies that the vacuum energy dominates over matter as z grows larger (bottom), which would violate the success of the standard Big Bang cosmology and therefore is not realistic.

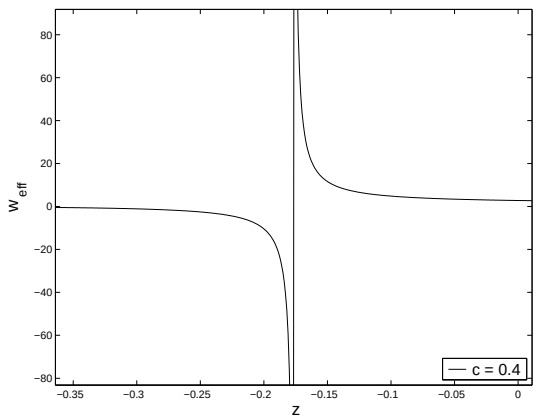

FIG. 7: The evolution of $w_{\rm eff}$. $L = R_{\rm ph}$. $\Omega_m = 0.3$, $\Omega_{r_c} = 0.12$ and $\epsilon = -1$. As the case shown in FIG.4, there exists a pole in the future evolution of the EoS, which implies the breakdown of the effective description.

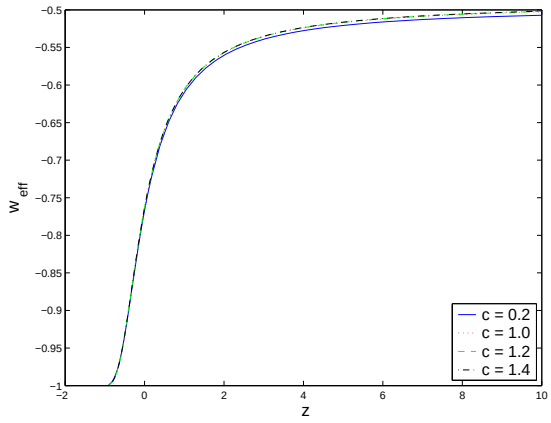

FIG. 8: The evolution of $w_{\rm eff}$. $L = R_{\rm eh}$. $\Omega_m = 0.3$, $\Omega_{r_c} = 0.12$ and $\epsilon = +1$

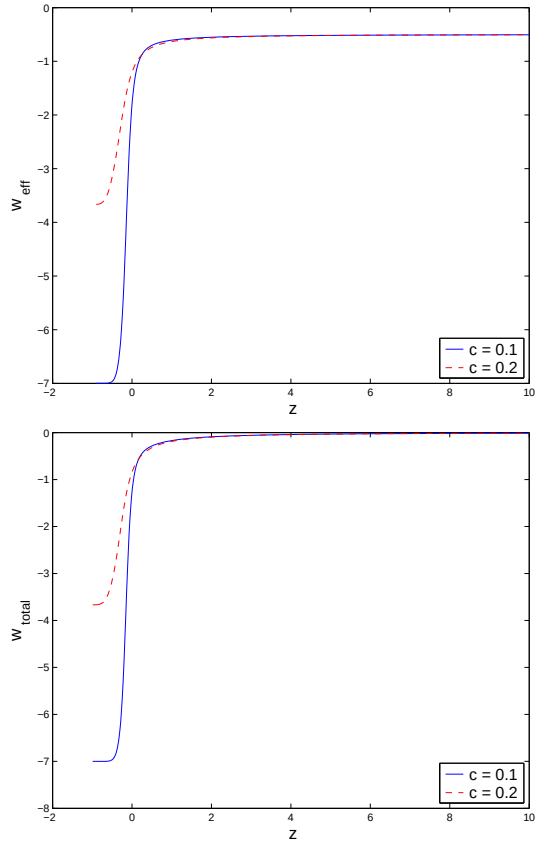

FIG. 9: The evolution of $w_{\rm eff}$. $L = R_{\rm eh}$, $\epsilon = +1$, $\Omega_m = 0.3$ and $\Omega_{r_c} = 0.06$.

a spatially flat universe it is defined by

$$D_L = (1+z)\int_0^z \frac{dz'}{E(z')}. \qquad (32)$$

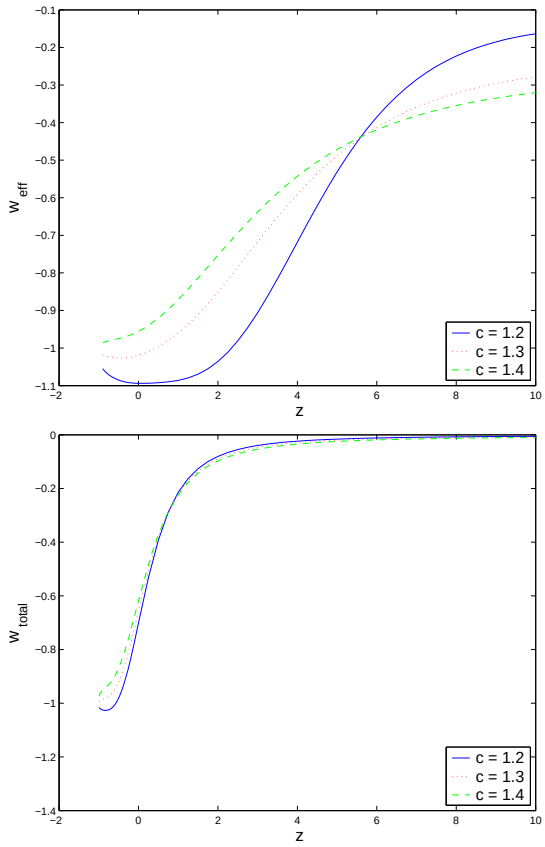

FIG. 10: The evolution of $w_{\rm eff}$. $L = R_{\rm eh}$, $\epsilon = -1$, $\Omega_m = 0.3$ and $\Omega_{r_c} = 0.12$. The effective EoS crosses -1, and since it dominates over matter in the future, the total EoS also crosses -1. This means that the future Big Rip singularity is not avoidable in this case.

The best fits are obtained by minimizing the quantity

$$\chi^2(\{\theta_k\}, \mathcal{M}) = \sum_i^{192} \frac{(\mu_{obs} - \mu_{th}(z_i; \{\theta_k\}, \mathcal{M})^2}{\sigma_i^2}, \qquad (33)$$

where σ_i are the observational uncertainties. We actually deal with the quantity χ^2 with the nuisance parameter marginalized over

$$\hat{\chi}^2 = -2\ln \int e^{-\chi^2/2} d\mathcal{M}. \qquad (34)$$

This is equivalent to minimize χ^2 with respect to $\mathcal{M}$[22], up to a negligible constant. One can easily show that χ^2 can be expanded in $\mathcal{M}$ around $\mathcal{M} = 0$ by

$$\chi^2(\{\theta_k\}, \mathcal{M}) = \chi^2(\mathcal{M} = 0, \{\theta_k\}) - 2B\mathcal{M} + C\mathcal{M}^2, \quad (35)$$

where

$$B = \sum_i^{192} \frac{\mu_{obs}(z_i) - \mu_{th}(z_i; \{\theta_k\}, \mathcal{M} = 0)}{\sigma_i^2}, \qquad (36)$$

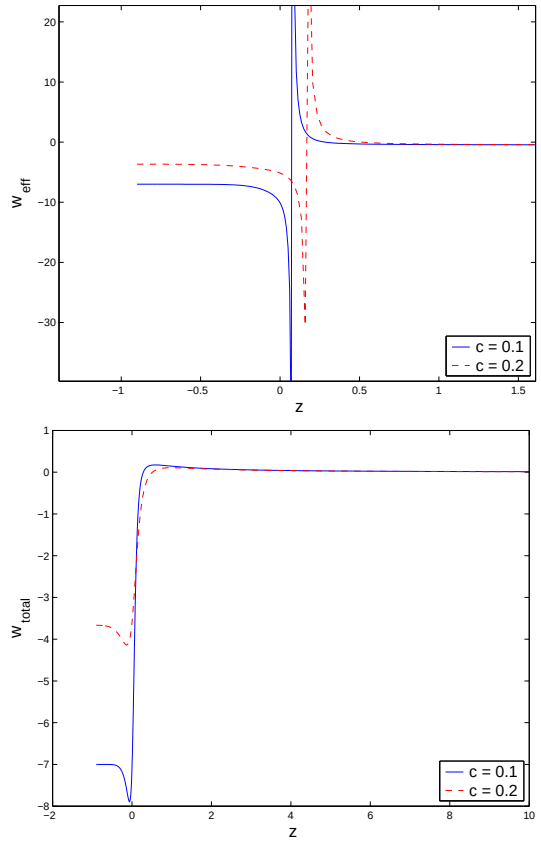

FIG. 11: The evolution of $w_{\rm eff}$. $L = R_{\rm eh}$, $\epsilon = -1$, $\Omega_m = 0.3$ and $\Omega_{r_c} = 0.06$.

$$C = \sum_i^{192} \frac{1}{\sigma_i^2}. \tag{37}$$

Obviously χ^2 becomes minimized if $\mathcal{M} = B/C$. Therefore, in practice we use

$$\chi^2_{SN}(\{\theta_k\}) = \chi^2(\mathcal{M} = 0, \{\theta_k\}) - \frac{B^2}{C} \tag{38}$$

as an alternative to $\hat{\chi}^2$ for the sake of efficiency in practical calculation without losing accuracy.

Another observational data we resort to as a complement to SNe data is from the observations of baryon acoustic oscillation peak(BAO). The acoustic oscillations in the relativistic plasma at the recombination epoch may imprint on the power spectrum of the non-relativistic matter of the late universe. And this acoustic signature in the large scale clustering of galaxies was detected by Eisenstein et al.[23] using a large sepctroscopic sample of the luminous red galaxies (LRGs) from the Sloan Digital Sky Survey (SDSS)[24]. We use the model-independent parameter A as given in[23]

$$A = \sqrt{\Omega_{m0}} z_1^{-1} [\frac{z_1}{E(z_1)} \int_0^{z_1} \frac{dz}{Ez}]^{1/3}, \tag{39}$$

where $z_1 = 0.35$ is the typical redshift of the LRGs. The measured value of A is 0.469 ± 0.017[23]. Correspondingly the quantity χ^2 is

$$\chi^2_{BAO} = \frac{(A - 0.469)^2}{0.017^2}. \tag{40}$$

And in the following we perform the joint analysis using $\chi^2 = \chi^2_{SN} + \chi^2_{BAO}$.

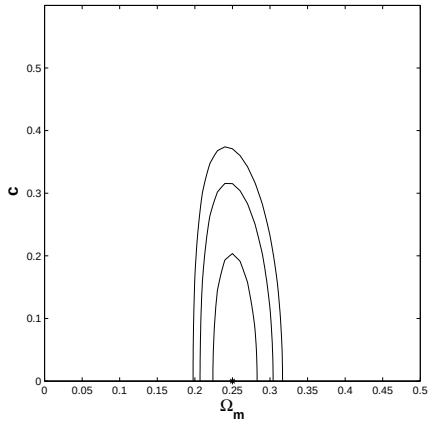

FIG. 12: Contour plot within 3σ from a joint analysis for $L = H^{-1}$ and $\epsilon = +1$. The best fits are $\Omega_{m0} = 0.25 \pm 0.02$ and $c = 0 + 0.14$.

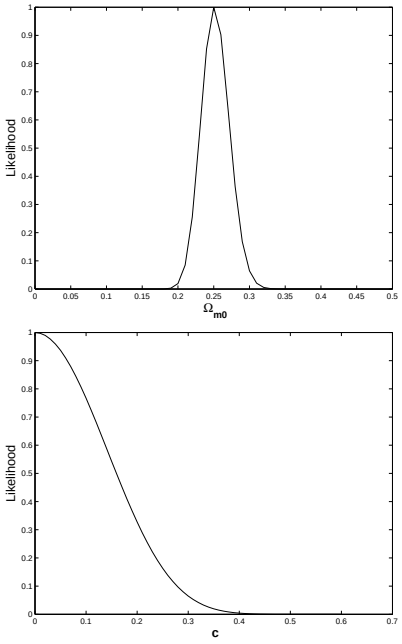

FIG. 13: Marginalized likelihood functions for Ω_{m0} and c.

For $L = H^{-1}$, there are two parameters (Ω_{m0}, c) to be fitted. And Ω_{r_c} is determined by Eq.(11). The result is shown in Fig.12. The best fits $\Omega_{m0} = 0.25$, $c = 0$

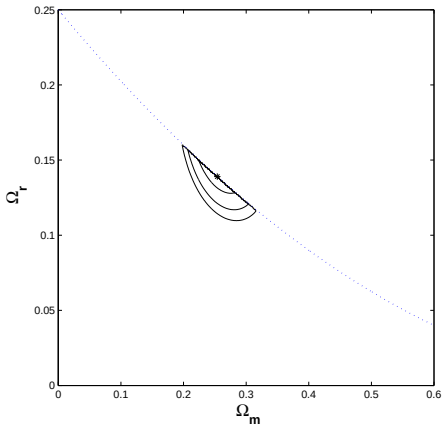

FIG. 14: Contour plot within 3σ from a joint analysis for $L = R_{\rm ph}$ and $\epsilon = +1$, with c marginalized. The best fits are $\Omega_{r_c} = 0.14 \pm 0.01$ and $\Omega_{m0} = 0.25 \pm 0.02$. The dotted line denotes the situation of $\Omega_{\Lambda 0} = 0$, above which $\Omega_{\Lambda 0} < 0$ and there the region is forbidden in our model.

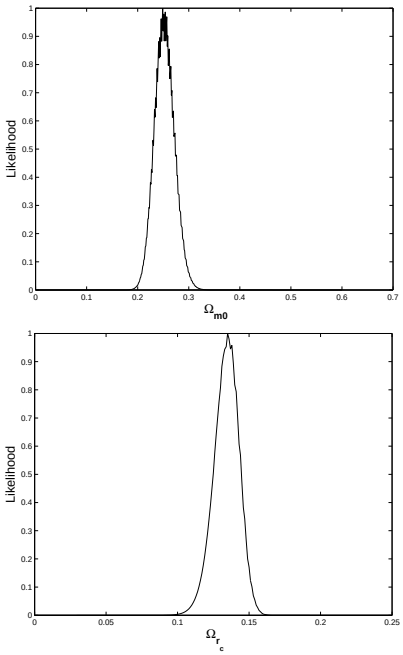

FIG. 15: Marginalized likelihood functions for Ω_{m0} and Ω_{r_c}.

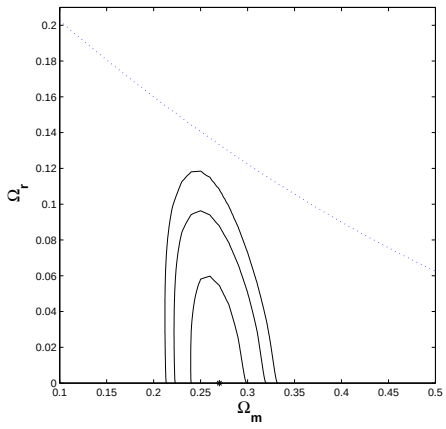

FIG. 16: Contour plot within 3σ from a joint analysis for $L = R_{\rm eh}$ and $\epsilon = +1$, with c marginalized. The best fits are $\Omega_{r_c} = 0 + 0.04$ and $\Omega_{m0} = 0.27 \pm 0.02$. Corresponding to the best fits, $c = 0.76$. Again, the dotted line denotes the boundary between $\Omega_{\Lambda 0} > 0$(below) and $\Omega_{\Lambda 0} < 0$(above).

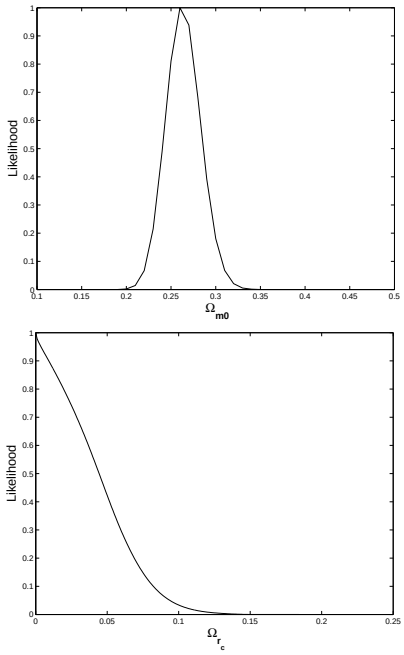

FIG. 17: Marginalized likelihood functions for Ω_{m0} and Ω_{r_c}.

and $\Omega_{r_c} = 0.14$ indicate that the observations prefer a pure DGP model without the holographic vacuum energy. This best fits are also consistent with those obtained in literature[25]. Fig.13 shows the marginalized likelihood function for the two parameters, in which the curve for Ω_{m0} is near-Gaussian whereas it is highly asymmetric for c due to the theoretical cutoff of this parameter. This leads to $\Omega_{m0} = 0.25 \pm 0.02$ and $c < 0.14$ within 68.3% confidence level.

For $L = R_{\rm ph}$, the results are given by Fig.14 and Fig.15, where we have marginalized the parameter c. In the contour plot, the dotted line represents $\Omega_{\Lambda 0} = 0$ in Eq.(19). Below this line $\Omega_{\Lambda 0} > 0$. In the region above $\Omega_{\Lambda 0} < 0$ and therefore it is the unphysical region for the parameters of the model. In the pure DGP model, the counterpart of Eq.(19) is

$$\Omega_k = 1 - 2\sqrt{\Omega_{r_c}} - \Omega_{m0}\,, \tag{41}$$

where Ω_k denotes the spatial curvature. If we identify $\Omega_{\Lambda 0}$ in Eq.(19) with Ω_k in Eq.(41), we find that our model

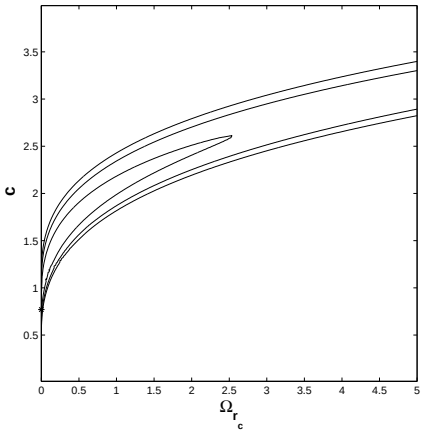

FIG. 18: Contour plot for $\Delta\chi^2 = 2.30, 6.17, 9.21$ from a joint analysis for $L = R_{\rm eh}$ and $\epsilon = -1$, with Ω_{m0} marginalized. The best fits are $\Omega_{r_c} = 0$, $c = 0.77$ denoted by a star on the plot. Corresponding to the best fits, $\Omega_{m0} = 0.27$.

TABLE I: Best fits

L	ϵ	$\Omega_{\rm m0}$	$\Omega_{\rm r_c}$	c	$w_{\rm eff0}$
H^{-1}	+1	0.25	0.14	0	-0.8000
$R_{\rm ph}$	+1	0.25	0.14	N/A	-0.7015
$R_{\rm eh}$	+1	0.27	0	0.76	-1.0828
$R_{\rm eh}$	−1	0.27	0	0.77	-1.0731

in this case is equivalent to the pure DGP model confined to a non-closed universe. The best fits are $\Omega_{r_c} = 0.14 \pm 0.01$ and $\Omega_{m0} = 0.25 \pm 0.02$, indicating a pure DGP model in a flat universe without vacuum energy.

For $L = R_{\rm eh}$, we have to consider the two branches. In the (+) branch, the results are shown in Fig.16 and Fig.17, with the parameter c marginalized. The best fits are $\Omega_{r_c} = 0 + 0.04$ and $\Omega_{m0} = 0.27 \pm 0.02$, correspondingly $c = 0.76$, indicating a pure holographic dark energy model with the negligible effect of higher dimensional gravity. In the (-) branch, as we can see from Fig.18 (with Ω_{m0} marginalized), the two outmost contours are not closed within a large region of the parameter space, indicating that current observations cannot impose tight constraint on the parameters in this case. Therefore the contours just represent the difference with respect to the minimum of χ^2, $\Delta\chi^2 = 2.30, 6.17, 9.21$ respectively, without an exact statistical meaning. Thus we do not present the likelihood plot as before. Despite of this, we can still get the best fits as $\Omega_{r_c} = 0$ and $c = 0.77$ with $\Omega_{m0} = 0.27$ correspondingly. This also indicates a pure holographic dark energy model.

IV. CONCLUSION

In this paper, we considered the evolution of the vacuum energy in the universe described by the DGP model. By numerically studying the EoS of the vacuum energy and the effective EoS of the combined effect of both vacuum energy and brane effect, we found that choosing the IR cut-off as the event horizon, the vacuum energy can drive the cosmic acceleration in both branches. In addition, the choice of the Hubble scale as the cut-off can also lead to the vacuum energy playing the role of dark energy. This is different from the case in ordinary 4D gravity, where $w_\Lambda < -1/3$ only when the event horizon is chosen as the IR cut-off. Further investigation shows that when $L = R_{\rm eh}$, the EoS may cross -1 and the vacuum energy would end up with a phantom phase, therefore the Big Rip singularity is inevitable, in contrast to the models such as LDGP[12] and SDGP[14] where only the effective EoS posses the crossing behavior and the total EoS is always larger than -1.

Through a joint analysis of SNe data and BAO data, the results of parameter fitting show that the DGP model with holographic vacuum energy can be consistent with the joint data constraints within 68.3% confidence level. For IR cut-off L as the Hubble scale and the particle horizon in the (+) branch, the best fits indicate that the observational data prefer a pure DGP model with negligible vacuum energy. For L as the event horizon in both branches, on the other hand, the best fits show a preference to the pure holographic dark energy model.

Acknowledgments

XW would like to thank Heng Yu and Xin Zhang for helpful discussions. XW and ZHZ were supported by the National Natural Science Foundation of China, under Grant No.10533010, 973 Program No.2007CB815401 and Program for New Century Excellent Talents in University (NCET) of China. RGC was supported in part by a grant from Chinese Academy of Sciences (No. KJCX3-SYW-N2), and by NSFC under grants No. 10325525, No. 10525060 and No. 90403029.

[1] A. G. Riess *et al.* [Supernova Search Team Collaboration], Astron. J. **116**, 1009 (1998) [astro-ph/9805201];
S. Perlmutter *et al.* [Supernova Cosmology ProjectCollaboration], Astrophys. J. **517**, 565 (1999) [astro-ph/9812133].

[2] D. N. Spergel *et al.* [WMAP Collaboration], [astro-ph/0603449];
L. Page *et al.* [WMAP Collaboration], [astro-ph/0603450];
G. Hinshaw *et al.* [WMAP Collaboration], [astro-ph/0603451];
N. Jarosik *et al.* [WMAP Collaboration],

[astro-ph/0603452].
[3] P. J. E. Peebles and B. Ratra, Rev. Mod. Phys. **75**, 559 (2003) [astro-ph/0207347];
S. M. Carroll, Living Rev. Rel. **4**, 1 (2001) [astro-ph/0004075];
S. Weinberg, Rev. Mod. Phys. **61**, 1 (1989).
[4] E. J. Copeland, M. Sami and S. Tsujikawa, Int. J. Mod. Phys. D **15**, 1753 (2006) [hep-th/0603057].
[5] S. Capozziello, S. Carloni and A. Troisi, [astro-ph/0303041];
S. Capozziello, V. F. Cardone, S. Carloni and A. Troisi, Int. J. Mod. Phys. D **12**, 1969 (2003);
S. M. Carroll, V. Duvvuri, M. Trodden and M. S. Turner, Phys. Rev. D **70**, 043528 (2004);
R. P. Woodard, astro-ph/0601672.
[6] G. Dvali, G. Gabadadze and M. Porrati, Phys. Lett. B **485**, 208 (2000);
G. R. Dvali, G. Gabadadze, M. Kolanovic and F. Nitti, Phys. Rev. D **64**, 084004 (2001) ;
G. R. Dvali, G. Gabadadze, M. Kolanovic and F. Nitti, Phys. Rev. D **65**, 024031 (2002).
[7] M. Li, Phys. Lett. B **603**, 1 (2004) [hep-th/0403127].
[8] A. Cohen, D.Kaplan and A. Nelson, Phys. Rev. Lett. **82**, 4971 (1999); [hep-th/9803132]
[9] S. D. H. Hsu, hep-th/0403052
[10] G. 't Hooft, [gr-qc/9310026];
L. Susskind, J. Math. Phys. 36, 6377 (1995) [hep-th/9409089]
[11] L. Randall and R. Sundrum, Phys. Rev. Lett. **83**, 4690 (1999);
L. Randall and R. Sundrum, Phys. Rev. Lett. **83**, 3370 (1999).
[12] V. Sahni and Y.Shtanov, JCAP **0311** (2003) 014 [astro-ph/0202346];
A. Lue and G. D. Starkman, Phys. Rev. D **70**, 101501 (2004) [astro-ph/0408246];
R. Lazkoz, R. Maartens and E. Majerotto, Phys. Rev. D **74**, 083510 (2006) [arXiv:astro-ph/0605701].
[13] L. P. Chimento, R. Lazkoz, R. Maartens and I. Quiros, JCAP **0609**, 004 (2006) [arXiv:astro-ph/0605450].
[14] Phys. Rev. D **75**, 023510 (2007) [astro-ph/0611834].
[15] M. Bouhmadi-López and R. Lazkoz, arXiv:0706.3896v1 [astro-ph]
[16] Q. G. Huang and Y. G. Gong, JCAP **0408**, 006 (2004) [astro-ph/0403590];
X. Zhang and F. Q. Wu, Phys. Rev. D **72**, 043524 (2005) [astro-ph/0506310];
Z. Chang, F. Q. Wu and X. Zhang, Phys. Lett. B **633**, 14 (2006) [astro-ph/0509531];
Z. L. Yi and T. J. Zhang, Mod. Phys. Lett. A **22**, 41 (2007) [astro-ph/0605596];
X. Zhang and F-Q. Wu, Phys. Rev. D **76**, 023502 (2007) [astro-ph/0701405].
[17] Davis *et al.* 2007 [astro-ph/0701510].
[18] M. Hamuy, M. M. Phillips, N. B. Suntzeff, R. A. Schommer and J. Maza, Astron. Jour. **112**, 2408 (1996) [astro-ph/9609064];
S. Jha, A. G. Riess and R. P. Kirshner, Astrophys. J. **659**, 122 (2007) [astro-ph/0612666].
[19] Wood-Vasey *et al.* 2007 [astro-ph/0701041].
[20] P. Astier *et al.*, Astron. Astrophys. **447**, 31 (2006) [arXiv:astro-ph/0510447].
[21] A. G. Riess *et al.*, Astrophys. J. **659**, 98 (2007) [arXiv:astro-ph/0611572].
[22] S. Nesseris and L. Perivolaropoulos, Phys. Rev. D **72**, 123519 (2005) [astro-ph/0511040];
L. Perivolaropoulos, Phys. Rev. D **71**, 063503 (2005) [astro-ph/0412308];
E. Di Pietro and J. F. Claeskens, Mon. Not. Roy. Astron. Soc. **341**, 1299 (2003) [astro-ph/0207332].
[23] D. J. Eisenstein, *et al.* ApJ 633, 560 (2005) [astro-ph/0501171].
[24] M. Tegmark *et al.* [SDSS Collaboration], Phys. Rev. D **69**, 103501 (2004) [astro-ph/0310723];
M. Tegmark *et al.* [SDSS Collaboration], Astrophys. J. **606**, 702 (2004) [astro-ph/0310725];
U. Seljak *et al.*, Phys. Rev. D **71**, 103515 (2005) [astro-ph/0407372];
J. K. Adelman-McCarthy *et al.* [SDSS Collaboration], Astrophys. J. Suppl. **162**, 38 (2006) [astro-ph/0507711];
K. Abazajian *et al.* [SDSS Collaboration], [astro-ph/0410239]; [astro-ph/0403325]; [astro-ph/0305492];
M. Tegmark *et al.* [SDSS Collaboration], Phys. Rev. D **74**, 123507 (2006) [astro-ph/0608632].
[25] C. Deffayet, Lett. B **502**, 199 (2001);
D. Jain, A. Dev & J. S. Alcaniz, Phys. Rev. D **66**, 083511 (2002);
J. S. Alcaniz, D. Jain & A. Dev, Phys. Rev. D **66**, 067301 (2002);
J. S. Alcaniz & Z. H. Zhu, Phys. Rev. D **71**, 083513 (2005);
Z. H. Zhu & J. S. Alcaniz, ApJ. **620**, 7 (2005);
N. Pires, Z. H. Zhu & J. S. Alcaniz, Phys. Rev. D **73**, 123530 (2006);
Z. K. Guo, Z. H. Zhu, J. S. Alcaniz & Y. Z. Zhang. ApJ. **646**, 1 (2006);
R. Maartens and E.Majerotto, Phys. Rev. D **74**, 023004 (2006) [astro-ph/0603353].